# Experimental investigation of vinyl chloride polymerization at high conversion: mechanism, kinetics and modelling

**T. Y. Xie, A. E. Hamielec*, P. E. Wood and D. R. Woods**
*Department of Chemical Engineering, Institute for Polymer Production Technology (MIPPT), McMaster University, Hamilton, Ontario, Canada L8S 4L7*
*(Received 19 October 1989; accepted 19 January 1990)*

The mechanism of vinyl chloride (VCM) polymerization is discussed in detail from both a chemical and a physical point of view. A comprehensive kinetic model for VCM bulk/suspension polymerization is developed based on all of the important elementary reactions for two-phase polymerization. A series of kinetic experiments covering an extensive temperature range with different initiator systems was carried out in an agitated 5 l batch reactor. Kinetic parameters were estimated by using these experimental data. The present model is in excellent agreement with experimental rate data measured in different laboratories and can be used to predict polymerization rate, conversion history and other kinetic features over the entire monomer conversion range.

**(Keywords: vinyl chloride; PVC; heterogeneous polymerization; mechanism; kinetics; modelling)**

## INTRODUCTION

The mechanism and kinetics of free radical bulk or suspension polymerization of vinyl chloride (VCM) have been extensively studied experimentally. VCM polymerization mechanisms proposed are based mainly on polymerization kinetics, chain microstructure and particle morphology studies. The extent and variety of research work dealing with the same problem reflects not only the great interest in, and extensive practical use of poly(vinyl chloride) (PVC), but also the complexity of VCM polymerization. The considerable experimental data in the literature reflects the pattern of VCM polymerization kinetics reasonably well, although a comprehensive kinetic model which can predict with adequate accuracy physical and chemical property changes during VCM polymerization has not been published to date.

In the present paper, the main contributions to the mechanisms and kinetics of VCM polymerization in terms of elementary chemical reactions, physical phenomena and kinetic modelling are reviewed. A comprehensive kinetic model which accounts for these elementary reactions, physical phenomena and reactor operational conditions for VCM polymerization over the entire conversion range is derived. Extensive kinetic experiments were done to evaluate the present model and to estimate kinetic and thermodynamic parameters. The main features of heterogeneous polymerization with diffusion-controlled reactions are accounted for quantitatively.

## MECHANISMS OF VCM POLYMERIZATION

### *Chemical reaction types*

A typical free radical polymerization mechanism includes initiation, propagation, chain transfer to small molecules and bimolecular termination steps. However, recent research has revealed that some reactions, such as chain transfer to monomer, involve more complicated mechanisms[1–9].

Initiation reactions have not been studied in detail. In kinetic modelling, it is assumed that initiation reactions occur in both monomer- and polymer-rich phases[10–17]. Lewis *et al.*[18] studied the sites of initiation and concluded that the main site of initiation at low conversions during VCM bulk polymerization is the continuous monomer phase. Marinin *et al.*[19] measured the decomposition rate constants of some peroxide initiators in the polymer phase under subsaturated pressure and found that the decomposition rate constant in the polymer phase can be significantly lower than that in the monomer phase. Important parameters for kinetic modelling, such as initiation efficiency, initiator partition coefficient and decomposition rate constant for VCM polymerization, have not been extensively studied in the literature.

The propagation reaction is considered to be mainly a head-to-tail addition of the monomer double bond to the radical centre[3,20]. However, the existence of a small number of head-to-head structures in PVC has been suggested earlier[21]. Rigo *et al.*[1] first proposed that the head-to-head propagation reaction causes the formation of chloromethyl branches in PVC. Bovey *et al.*[3] gave evidence for the presence of this structure by $^{13}C$ nuclear magnetic resonance (n.m.r.) measurements on reduced PVC. Starnes *et al.*[4,5] provided further evidence for the proposed mechanism. This mechanism can more reasonably explain how chain transfer to monomer occurs during free radical polymerization of VCM. Hence propagation reactions can involve several types of radicals in addition to the most common radical type as shown in *Figure 1*.

Chain transfer to monomer plays a very important role in controlling molecular weight development in VCM

* To whom correspondence should be addressed

0032-3861/91/030537-21

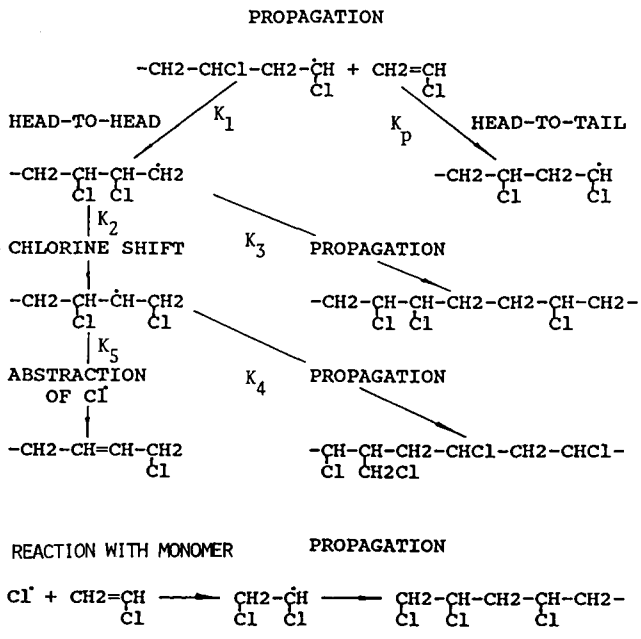


**Figure 1** Mechanism of radical transfer to monomer and formation of some defect structures of PVC

polymerization. In classical kinetic studies of VCM polymerization, chain transfer to monomer was considered to involve a polymer chain transferring its radical centre to monomer directly[22–28] by abstraction of a chlorine or hydrogen from the VCM[24,27]. However, the unsaturated end groups formed by this chain transfer mechanism cannot be found by n.m.r. measurements[29,30]. Therefore, Caraculacu *et al.*[29,30] suggested that transfer to monomer would be realizable only by abstracting an atom from a high energy structure such as from head-to-head addition polymer radicals, the monomer being the acceptor. Detailed n.m.r. measurements showed that chain transfer to monomer involves a more detailed mechanism as shown in *Figure 1*. As mentioned above, the head-to-head addition was proposed by Rigo *et al.*[1]. The chlorine abstraction step was suggested by Bezdaea *et al.*[2], while Caraculacu *et al.*[29,30] and Starnes *et al.*[4,5] suggested the subsequent chlorine addition to the monomer double bond. Hjertberg *et al.*[9] suggested that the chlorine atoms which result from head-to-head addition abstract hydrogen atoms from the polymer backbone and this results in the formation of internal double bonds or long chain branches. The mechanism of chain transfer to monomer is supported by the following findings:

(1) the major part of the unsaturated chain ends has 1-chloro-2-alkene structure[7,31,32];

(2) the major part of the saturated chain ends consists of the 1,2-dichloro-alkane structure[4,7,8,31,32]; and

(3) the presence of chloromethyl branches[3–6,33–35].

Clearly, the classical mechanism involving macroradical direct chain transfer to monomer is not valid for VCM polymerization.

Whether the bimolecular termination reaction between polymer radicals is combination or disproportionation is difficult to determine because of the significance of chain transfer to monomer in this system. Razuvayev *et al.*[36] were first to investigate the mechanism of bimolecular termination in the free radical polymerization of VCM by $^{14}C$-labelled initiators. It was found that, in the bulk and suspension polymerization of VCM, the average number of initiator end groups per polymer molecule is 0.19–0.40, i.e. a maximum of 19–40% of the polymer molecules are produced by bimolecular termination reaction. Park *et al.*[37] studied solution polymerization of VCM using $^{14}C$-labelled initiator and found that 25% of bimolecular termination occurs by combination and 75% by disproportionation. Hence a maximum 5–10% of the polymer molecules are produced by combination termination. Note that the resulting structure by combination termination is similar to that by head-to-head addition. But the content of head-to-head structure is so low that it cannot be detected by $^{13}C$-n.m.r.[4]. Hjertberg *et al.*[38] estimated the head-to-head structure to be less than 0.2 per 1000 monomeric units using a chemical method. Assuming the degree of polymerization to be 1000, one may estimate that there is a maximum of 20% of the polymer molecules with one head-to-head structure. Therefore, 10–15% of the polymer molecules experience one head-to-head followed by tail-to-tail propagation addition.

In addition to bimolecular termination and propagation, macroradicals experience other reactions, including chain transfer to polymer, intramolecular chain transfer or back-biting reactions[6,32,39]. All these reactions result in short or long chain branches. Primary radical termination may also occur in VCM polymerization[40–42]. However, the significance of this reaction for the calculation of total radical concentration is uncertain.

All of the chemical reactions which have been identified by kinetic and microstructural studies and are important for kinetic and reactor modelling are now summarized.

*Initiation*

| | | |
|---|---|---|
| 1 | $I \xrightarrow{K_d} R_i^{\bullet}$ | decomposition of initiator |
| 2 | $R_i^{\bullet} \xrightarrow{K_i} R_i^{\bullet}$ | generation of polymer radicals |

*Propagation and chain transfer reactions*

| | | |
|---|---|---|
| 3 | $R_r^{\bullet} + M \xrightarrow{K_p} R_{r+1}^{\bullet}$ | head-to-tail propagation |
| 4 | $R_r^{\bullet} + M \xrightarrow{K_1} R_{r+1}^{\bullet *}$ | head-to-head propagation |
| 5 | $R_r^{\bullet *} \xrightarrow{K_2} (R_r^{\bullet *})'$ | chlorine shift reaction |
| 6 | $R_r^{\bullet *} + M \xrightarrow{K_3} R_{r+1}^{\bullet}$ | tail-to-tail propagation |
| 7 | $(R_r^{\bullet *})' + M \xrightarrow{K_4} R_{r+1}^{\bullet}$ | formation of chloromethyl branches |
| 8 | $(R_r^{\bullet *})' \xrightarrow{K_5} P_r + Cl^{\bullet}$ | splitting off $Cl^{\bullet}$ |
| 9 | $Cl^{\bullet} + M \xrightarrow{K_p} R_1^{\bullet}$ | initiation of polymer radicals by $Cl^{\bullet}$ |
| 10 | $Cl^{\bullet} + P_r \xrightarrow{K_{fp}} R_r^{\prime\prime} + HCl$ | $Cl^{\bullet}$ transfer to polymer |

| | | |
|---|---|---|
| 11 | $R_r^{\prime\prime} + M \xrightarrow{K_p} R_{r+1}^{\bullet}$ | propagation towards formation of a chain branch |
| 12 | $R_r^{\prime\prime} \xrightarrow{K_e} P_r + Cl^{\bullet}$ | formation of an internal double bond |
| 13 | $R_r^{\bullet} + P_s \xrightarrow{K_{fp}} R_s^{\prime\prime} + P_r$ | chain transfer to polymer |
| 14 | $R_s^{\prime\prime} + M \xrightarrow{K_p} R_{s+1}^{\bullet}$ | formation of long chain branch |
| *Termination* | | |
| 15 | $R_r^{\bullet} + R_s^{\bullet} \xrightarrow{K_{tc}} P_{r+s}$ | combination |
| 16 | $R_r^{\bullet} + R_s^{\bullet} \xrightarrow{K_{td}} P_r + P_s$ | disproportionation |
| 17 | $R_r^{\bullet} + R_i^{\bullet} \xrightarrow{K_{ti}} P_r$ | primary radical termination |
| 18 | $R_r^{\bullet} + Cl^{\bullet} \xrightarrow{K_{tCl}} P_r$ | termination with $Cl^{\bullet}$ |
| *Other reactions* | | |
| 19 | $R_r^{\bullet} \xrightarrow{K_b} R_{r,b}^{\bullet}$ | back-biting reaction |
| 20 | $R_{r,b}^{\bullet} + M \xrightarrow{K_p} R_{r+1,b}^{\bullet}$ | propagation towards formation of a short branch |

All the reactions shown above may occur in both monomer and polymer phases simultaneously. A kinetic model involving all these chemical reactions has not been reported to date. In the present model development, these elementary reactions will be considered and their effects on polymerization rate discussed in detail.

*Physical phenomena*

Because PVC is effectively insoluble in its own monomer, VCM polymerization is a heterogeneous process which involves several physical transitions throughout the course of polymerization. The final PVC product of bulk or suspension polymerization is made up of primary particles and their agglomerates. For valid kinetic modelling it is necessary to understand the mechanisms for formation, growth and aggregation of primary particles.

The formation of primary particles has been studied by many investigators[43–59]. Based on turbidimetric measurements, Boissel *et al.*[48] found that polymer precipitates from the monomer phase at conversions as low as 0.001%. This value is much lower than that (0.03% solubility of PVC in monomer at ambient temperature) measured by Ravey *et al.*[60]. Cotman *et al.*[43] estimated that macroradicals become insoluble in the monomer at a degree of polymerization of 25–32. Rance *et al.*[54] recently suggested that the solubility of polymer in the monomer is limited to polymer chains containing 10 monomer units or fewer based on the Flory interaction parameter. Although the range of these values is large, they do indicate that phase separation during VCM polymerization occurs at a very low conversion. The first particles which appear at these low conversions are so called microdomains, which are 0.01–0.02 $\mu$m in diameter. They are believed to result from precipitation and coagulation of single polymer radicals. Their lifetimes are $<30$ s and, therefore, cannot be measured by photon correlation spectroscopy methods[54]. The aggregation of microdomains produces domains (primary particle nuclei, 0.1–0.3 $\mu$m in diameter), the first observable entities of the new monomer swollen polymer phase[47–54,61–63]. Willmouth *et al.*[55] and, more recently, Tornell *et al.*[64] studied the conversion dependence of particle size and number density at earlier stages of polymerization. From information in the literature, one can conclude that a domain is formed and grows by the following processes:

(1) aggregation of microdomains;
(2) precipitation of macroradicals and macromolecules (chain length $r > r_c$) on the formed microdomain or domain; and
(3) polymerization inside the microdomain or domain.

These three processes occur simultaneously during the early stages of polymerization.

Further aggregation or growth of domains results in the formation of primary particles. The primary particles grow with conversion at almost the same rate[43–46,49,65]. The average diameter of primary particles is $\approx$0.8–1.0 $\mu$m. Much of the existing work on grain formation has involved studies of the very early stages of the process or over a narrow conversion range. Recently, Smallwood[66] studied the later stages of the polymerization process at commercial polymerization temperatures (51–71°C). PVC samples were taken at 5–85% conversion. A series of scanning electron micrographs shows that the primary particles increase in size until 50–70% conversion, depending on reaction temperature. Then the primary particles fuse together at higher conversions (aggregation of primary particles has occurred since low conversion). By examining those results[66], one may find that the primary particles increase in size with conversion until the free monomer phase disappears. Hence, one can conclude that the primary particles grow by accretion of microdomains or domains onto their surface and polymerization inside the primary particles.

The limiting size of primary particle is $\approx 1.4$ $\mu$m and the final number of primary particles is $\approx 2.0 \times 10^{11}$ $cm^{-3}$ for all reaction temperatures (51–71°C)[66].

Wilson *et al.*[50] and Davidson *et al.*[53] demonstrated that the primary particles carry negative charges which may result from the presence of HCl formed during polymerization (see reaction 10).

As the primary particles increase in size and the volume fraction of the polymer phase increases, aggregation will involve multiparticle contacts. Thus aggregation will result in a decrease in primary particle number and in the formation of a continuous network of primary particles throughout the polymer particle/monomer droplet. The continuous network is likely to form at between 10 and 30% conversion[66]. According to Smallwood's results[66], after the monomer phase disappears, further polymerization leads to fusion of primary particles and formation of agglomerates. Hence, at high conversion, only agglomerates of primary particles can

be seen, and their size strongly depends on reaction temperature.

In view of the preceding observations, one can summarize the mechanism of formation of PVC grains as follows.

*Stage 1.* Macroradicals or macromolecules with chain length more than a critical value $r_c$ begin to precipitate from the monomer phase (at $\approx 0.001\%$ conversion).

*Stage 2.* Aggregation of macroradicals and macromolecules after precipitation produces microdomains (0.01–0.02 $\mu$m, at $<0.01\%$ conversion). The microdomain is not well defined.

*Stage 3.* Aggregation of microdomains produces domains (0.1–0.3 $\mu$m, $<1\%$ conversion) stabilized by negative charge. This stage is completed at 5–10% conversion.

*Stage 4.* Aggregation and growth of domains causes formation of primary particles until the formation of continuous networks in droplets (about 15–30% conversion).

*Stage 5.* Primary particles grow and aggregate until free monomer phase disappears; the diameter of final primary particles is $\approx 1.2$–1.5 $\mu$m (50–70% conversion).

*Stage 6.* Primary particles fuse together as agglomerates (5–10 $\mu$m) until the limiting conversion is reached.

There is no clear boundary line between stages; two neighbouring stages may occur simultaneously during polymerization. Allsopp[67,68] proposed a schematic representation of the mechanism of VCM polymerization. With recent findings in mind, we suggest a modified scheme of the mechanism of VCM polymerization as shown in *Figure 2*.

*Dynamics and modelling of VCM polymerization*

The dynamics of VCM polymerization processes as a whole has not been studied comprehensively. Meeks[69] first measured conversion, polymerization heat and rate, reactor pressure, cooling water temperature and flow rate simultaneously as a function of polymerization time. Recently, Nilsson *et al.*[70] measured polymerization rate, reactor pressure and amount of liquid monomer as a function of conversion in suspension and emulsion polymerization systems. In most of the kinetic studies, only conversion change with time was measured.

Based on data in the literature, one can summarize the

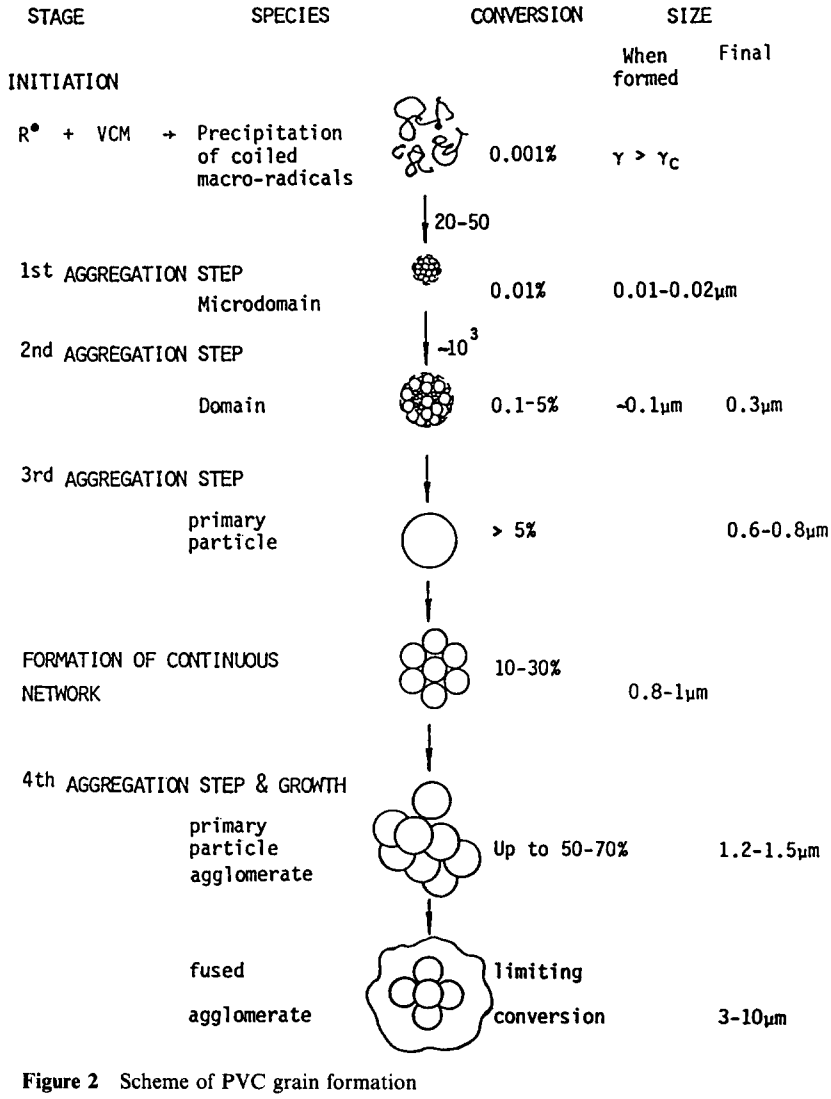


**Figure 2** Scheme of PVC grain formation

main dynamic features of VCM polymerization as follows:

(1) The polymerization rate increases with conversion at a low critical conversion, i.e. the so-called auto-acceleration[12–15,22,25,28,43,60,69,71–84]. The maximum rate of polymerization occurs just after the reactor pressure starts to drop[69,70]. Then the polymerization rate decreases dramatically with conversion[13,60,69,70,84]. The polymerization rate effectively decreases to zero before 100% conversion of monomer at commercial polymerization temperatures.

(2) The reactor pressure, for isothermal polymerization, remains constant until a certain high conversion and then the pressure decreases gradually with conversion[69,70,85]. The pressure may start to drop slowly before the monomer phase disappears[70]. The same phenomenon was noticed in our recent laboratory experiments.

(3) The reaction order with respect to initiator concentration is between 0.5 and 0.8[13,15,22,40,43,71,79,80,84,86,87]. These results were based on relatively low conversion rate measurements.

(4) The molecular weight of PVC does not strongly depend on monomer conversion or initiator concentration[11,13,22,71,88], but it increases with decreasing polymerization temperature[13]. At very high conversions, the molecular weight decreases with conversion[89].

(5) Chain transfer to monomer plays a dominant role in controlling molecular weight[13]. The ratio of the chain transfer to monomer rate constant to the propagation rate constant is as large as $1.0–5.0 \times 10^{-3}$ at commercial polymerization temperatures[13,15,27,43,71,79]. According to the new mechanism of chain transfer to monomer, this value is for a group of kinetic rate constants. This will be discussed later.

A comprehensive kinetic/reactor model which can describe these dynamic features of VCM polymerization has not been reported to date. Most kinetic studies to date have emphasized polymerization rate modelling.

Based on the pertinent phenomena of VCM polymerization above, one knows that phase separation occurs at very low monomer conversions. For kinetic modelling, therefore, it is reasonable to assume that polymerization occurs in the monomer and polymer phases simultaneously from the very beginning of the polymerization. The solubility of PVC in monomer is so low ($\approx 0.001\%$) that the monomer phase is considered to be essentially pure monomer, while the polymer phase is swollen with about 30% monomer. As the reaction proceeds, the mass of the monomer phase decreases while that of the polymer phase grows, but the composition of each phase is essentially constant[10,71], because the rate of monomer diffusion into polymer particles is sufficiently high to ensure equilibrium during polymerization with a constant equilibrium concentration of monomer in the particles[14] before the monomer phase is consumed. As long as VCM exists as a separate phase, it will exert its own vapour pressure and the pressure in the reactor will be essentially constant during isothermal polymerization. When conversion reaches a value $X_f$ the pressure in the reactor begins to drop[85] and polymerization proceeds in the polymer phase until a limiting conversion is reached. Therefore, a model valid for the entire conversion range must describe two-phase polymerization before and single phase polymerization after conversion $X_f$.

When conversion is $< X_f$, the following equations apply for a batch reactor:

$$-\frac{dN_m}{dt} = K_{p1}[M]_1[R^\bullet]_1 V_1 + K_{p2}[M]_2[R^\bullet]_2 V_2 \quad (1)$$

If $K_{p1} = K_{p2} = K_p$, then equation (1) becomes

$$-\frac{dN_m}{dt} = K_p[M]_1[R^\bullet]_1 V\left[1 + \left(\frac{[M]_2[R^\bullet]_2}{[M]_1[R^\bullet]_1} - 1\right)\phi_2\right] \quad (2)$$

where $K_p$ depends only on temperature; $[M]_1$ and $[M]_2$ are also constant and $[M]_1 > [M]_2$ when $X < X_f$; $[R^\bullet]_1$ will decrease gradually due to decrease in initiator concentration; the total volume $V$ will decrease due to the larger polymer density; the polymer phase volume fraction $\phi_2$ is positive ($\phi_2 < 1.0$) and will increase gradually with conversion. Considering typical polymerization rate profiles, one may conclude that only the following condition can be true:

$$\frac{[M]_2[R^\bullet]_2}{[M]_1[R^\bullet]_1} - 1 > 0 \quad (3)$$

or

$$[R^\bullet]_2/[R^\bullet]_1 > [M]_1/[M]_2 > 1 \quad (4)$$

Therefore, the following inequality is always true for VCM polymerization:

$$[R^\bullet]_2 > [R^\bullet]_1 \quad (X < X_f) \quad (5)$$

It is clear that to develop a valid model for rate of polymerization the most important task is properly to express $[R^\bullet]_2/[R^\bullet]_1$ as a function of the variables which are known or can be measured experimentally. This is the main reason why most kinetic models differ according to the relations used for radical concentrations in the two phases.

Although polymerization in the polymerization phase was suggested earlier (Reference 44 and references therein), Talamini[10,71] first proposed a two-phase polymerization scheme and modelling approach. The major assumption in Talamini's model was setting $[R^\bullet]_2/[R^\bullet]_1$ constant ($= P$). An oversimplified model with adjustable parameter $P$ was thus derived. The following important factors were neglected in Talamini's model: unequal initiator partition between the two phases; consumption of initiator; volume shrinkage due to the density difference between VCM and PVC; and radical migration between the two phases.

Abdel-Alim *et al.*[13] modified Talamini's model by considering reaction volume change and initiator consumption and first extended the model to conversions above $X_f$. But unequal initiator partition and radical migration were neglected in the model.

To modify Talamini's model, Ugelstad *et al.*[12,82] proposed radical exchange between the two phases. But Ugelstad *et al.* over-emphasized the importance of absorption and desorption of radicals and still assumed a constant value for $[R^\bullet]_2/[R^\bullet]_1$. Therefore, the kinetic model remains the same in form but gives a different explanation for magnitude of the ratio $[R^\bullet]_2/[R^\bullet]_1$.

Kuchanov *et al.*[14] considered that the desorption of radicals from the polymer phase can be ignored because only a small fraction of the radicals with short chain lengths can desorb from the polymer phase. They further assumed that the ratio of mole fraction of initiator in both phases remains constant. Unfortunately, they only compared the model predictions with low conversion

data. However, when the authors extended the model to high conversions (>77%), they still considered the monomer as a separate phase. This seems to contradict the observed physical phenomena discussed earlier.

Olaj[15] further assumed that all of the radicals formed in the monomer phase transfer to the polymer phase, i.e. there is no termination reaction in the monomer phase. Hence, in Olaj's model, the reaction order with respect to initiator concentration is 1.0, which is higher than that observed experimentally.

More recently, Suresh *et al.*[16] proposed a concept 'kinetic solubility', which assumes that rapidly growing polymer chains have considerably greater solubility than the thermodynamic solubility of preformed polymer molecules of the same size and so can remain in solution even under thermodynamically unfavourable conditions. In the model development, radical precipitation and transfer to monomer were considered, but radical termination in the monomer phase was neglected. Hence the rate equation has features which are similar to Olaj's model.

Kelsall *et al.*[17] considered the unequal partition of initiator between the two phases and derived model equations. During their simulation of VCM polymerization, radical migration between phases was treated as a mass transfer process. The validity of their model has not been examined experimentally.

In view of these observations, one can conclude that polymerization in two phases is commonly accepted. The significance of radical migration between the two phases still remains unclear. The main ideas for a two-phase model are summarized in *Figure 3*.

Very few studies of the kinetics of polymerization at high conversions ($X > X_f$) have been made. Abdel-Alim *et al.*[13] first extended the two-phase model to single phase polymerization at high conversions. More recently, Kelsall *et al.*[17] simulated VCM polymerization to high conversion levels. Hamielec *et al.*[90] first accounted for diffusion-controlled bimolecular termination and propagation at high conversions. In fact, sufficient experimental kinetic data for high conversions ($X > X_f$) have not accumulated in the literature to test comprehensively the validity of existing kinetic models.

Although the quality of kinetic modelling has steadily improved, none of the existing models is directly applicable to commercial processes for the following main reasons:

(1) reactor operation conditions have not been considered in the kinetic modelling;

(2) diffusion controlled bimolecular termination and propagation and initiation efficiency in the polymer phase have not been studied in detail, particularly at the higher monomer conversion levels which are commercially important; and

(3) valid kinetic parameters have not been estimated for VCM polymerization over the entire conversion range.

For the present kinetic model development, we pay attention to the entire conversion range and particularly emphasize high conversion levels. Extensive kinetic

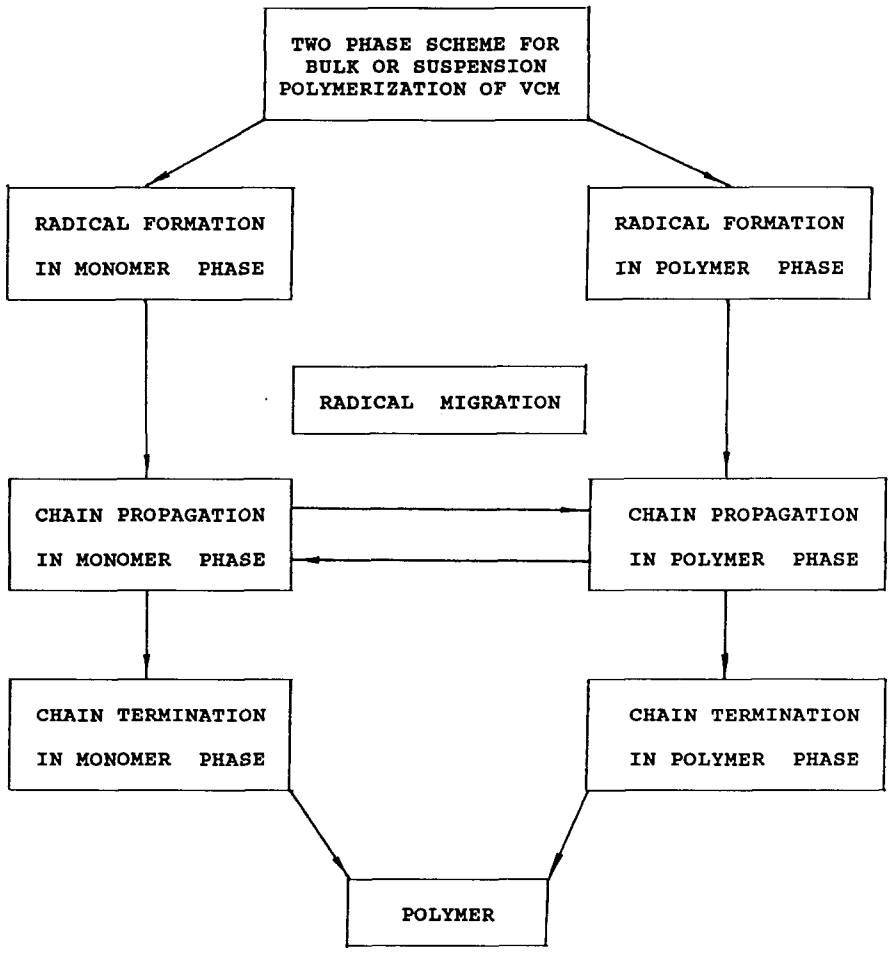


**Figure 3** Radical history for VCM polymerization

experiments, covering the commercial reaction temperature range, were made to evaluate the model and estimate valid kinetic parameters.

## MODEL DEVELOPMENT

The kinetic mechanisms of VCM polymerization discussed above will be accounted for in the present model. The following assumptions are made in the model development.

(1) Polymerization of VCM in the water and vapour phases is negligible.

(2) Polymerization of VCM proceeds in two phases – monomer and polymer phases – when conversion is $< X_f$. When conversion is $> X_f$, polymerization proceeds in the polymer phase.

(3) Polymer radicals can transfer from the monomer phase into the polymer phase by precipitation and capture. Transfer of polymer radicals in the reverse direction is limited to small radicals with $r < r_c$. Instantaneous equilibrium with respect to transfer of mobile radicals between monomer and polymer phases is assumed.

(4) Monomer and initiators diffuse into and out of the polymer phase rapidly so that equilibrium partition of these species is assumed at all times.

(5) Bimolecular termination of polymer radicals in the monomer phase is chemically controlled, but bimolecular termination in the polymer phase is diffusion controlled over the entire conversion range. Propagation reactions are also diffusion controlled at $X > X_f$ and initiator efficiency falls rapidly at high monomer conversion due to a large increase in radical recombination in the cage ('cage effect').

If the long chain approximation is considered valid for both monomer and polymer phase, with the assumptions above, the polymerization rate in terms of conversion per unit time can be expressed as

$$\frac{dX}{dt} = \frac{K_p}{N_0 M_m}([R^\bullet]_1 M_1 + [R^\bullet]_2 M_2) \tag{6}$$

where $N_0$ is the initial number of moles of VCM, $M_m$ is molecular weight of VCM, and $M_1$ and $M_2$ are the weights of monomer in the monomer and polymer phases, respectively (which can be expressed as a function of conversion and reactor operation conditions[85]).

Strictly, all of the radicals consuming monomer should be included in $[R^\bullet]_1$ and $[R^\bullet]_2$. However, according to the microstructure of ordinary PVC[91], the structure due to initiation reactions (2) and (9) is about one unit per polymer molecule and hence monomer consumption due to these reactions is negligible. Similarly, monomer consumption due to head-to-head and tail-to-tail propagation is <0.02%. Therefore, the long chain approximation is valid for VCM polymerization. It is assumed that radical centres forming short and long chain branches have the same reactivity as radical centres on chain ends. Hence $[R^\bullet]_1$ and $[R^\bullet]_2$ include radicals on chain ends and polymer backbone radicals. From the conversion rate point of view, this treatment is valid. However, these radical types have to be considered individually for PVC molecular weight and microstructure modelling.

Radical and monomer concentrations, initiation rate and kinetic parameters are essential factors in any polymerization rate expression. These factors are now discussed separately.

*Radical concentrations*

From the previous section, one knows that the radical concentration in the polymer phase is much greater than that in the monomer phase. It is assumed that there is no mass transfer of radicals from the monomer phase to the polymer phase when the chain length $r < r_c$ (chain length at which macroradicals start to precipitate from the monomer phase). Radicals with $r \geqslant r_c$ can transfer from the monomer to the polymer phase by precipitation and capture. On the other hand, desorption of radicals from the polymer phase is limited to the radicals with chain length $< r_c$. Thus the total radical balance for the two phases can be expressed as follows:

$$\begin{aligned}\frac{d(R^\bullet)_1}{V_1\,dt} &= R_{I1} + K'_p[Cl^\bullet]_1[M]_1 - K_{p1}[M]_1[R^\bullet_{r_c-1}]_1 \\ &\quad - K'_{t1}[R^\bullet]_1([R^\bullet_1] + [Cl^\bullet]_1) - K_5[R^{\bullet *\prime}]_1 \\ &\quad - K_{t1}[R^\bullet]_1^2 + K_{de}\sum_{r=1}^{n}[R^\bullet_r]_2 V_2/V_1 \\ &= 0\end{aligned} \tag{7}$$

$$\begin{aligned}\frac{d(R^\bullet)_2}{V_2\,dt} &= R_{I2} + K_{p1}[M]_1[R^\bullet_{r_c-1}]_1 V_1/V_2 \\ &\quad + K'_{p2}[Cl^\bullet]_2[M]_2 + K'_{fp}[Cl^\bullet]_2(Q_1)_2 \\ &\quad - K'_{t2}[R^\bullet]_2([R^\bullet_1]_2 + [Cl^\bullet]_2) - K_5[R^{\bullet *\prime}]_2 \\ &\quad - K_{de}\sum_{r=1}^{n}[R^\bullet_2]_2 - K_{t2}[R^\bullet]_2^2 \\ &= 0\end{aligned} \tag{8}$$

where

$$(R^\bullet)_i = \sum_{r=1}^{\infty}(R^\bullet_r)_i + \text{backbone radicals} \quad (i = 1, 2)$$

and $n < r_c$.

Based on the reaction mechanisms shown in the previous section, the radical concentrations $[R^\bullet_1]_2$, $[Cl^\bullet]$, $[R^{\bullet\prime}]$, $[R^{\bullet *}]$, $[R^{\bullet *\prime}]$, $[R^\bullet_i]$ and $[R^\bullet_r]_2$ can be expressed in the following steady-state equations:

$$\begin{aligned}\frac{dR^\bullet_1}{V_2\,dt} &= R_{I2} + K'_p[Cl^\bullet]_2[M]_2 - K_p[M]_2[R^\bullet_1]_2 \\ &\quad - K_{t2}[R^\bullet]_2[R^\bullet_1]_2 - K_{de}[R^\bullet_1]_2 \\ &= 0\end{aligned} \tag{9}$$

$$\begin{aligned}\frac{d(Cl^\bullet)_1}{V_1\,dt} &= K_5[R^{\bullet *\prime}]_1 + K_{e1}[R^{\bullet\prime}]_1 + K_{de}[Cl^\bullet]_2 \\ &\quad - K'_{p1}[Cl^\bullet]_1[M]_1 - K'_{fp}[Cl^\bullet]_1(Q_1)_1 \\ &= 0\end{aligned} \tag{10}$$

$$\begin{aligned}\frac{d(Cl^\bullet)_2}{V_2\,dt} &= K_5[R^{\bullet *\prime}]_2 + K_{e2}[R^{\bullet\prime}]_2 - K_{de}[Cl^\bullet]_2 \\ &\quad - K'_{p2}[M]_2[Cl^\bullet]_2 - K'_{fp}[Cl^\bullet]_2(Q_1)_2 \\ &= 0\end{aligned} \tag{11}$$

$$\begin{aligned}\frac{dR^{\bullet\prime}_i}{V_i\,dt} &= K'_{fpi}[Cl^\bullet]_i(Q_1)_i - K_{pi}[R^{\bullet\prime}]_i[M]_i - K_e[R^{\bullet\prime}]_i \\ &= 0\end{aligned} \tag{12}$$

$$\frac{dR^{**}}{V_i dt} = K_1[M]_i[R^*]_i - K_2[R^{**}]_i - K_3[R^{**}]_i[M]_i = 0 \quad (13)$$

$$\frac{dR^{**'}}{V_i dt} = K_2[R^{**}]_i - K_4[R^{**'}]_i[M]_i - K_5[R^{**'}]_i = 0 \quad (14)$$

$$\frac{dR_i^*}{V_i dt} = R_{Ii} - K_{ii}[M]_i[R_i^*]_i - K'_{ti}[R^*]_i[R_i^*]_i = 0 \quad (15)$$

$$\frac{dR_r^*}{V_2 dt} = K_{p2}[M]_2[R^*_{r-1}]_2 - K_{t2}[R_r^*]_2[R^*]_2 = 0 \quad (16)$$

where $i = 1, 2$, indicating monomer and polymer phases respectively. The phase subscripts for $K_1$, $K_2$, $K_3$, $K_4$, $K_5$ are dropped for simplicity.

From equation (12), one has

$$[R^{*'}]_i = \frac{K'_{fpi}[Cl^*]_i(Q_1)_i}{K_{pi}[M]_i + K_{ei}} \quad (i = 1, 2) \quad (17)$$

Because solubility of PVC in the monomer is very low, $(Q_1)_1$ is negligible, so that $[R^{*'}]_1$ can be neglected.

Equation (13) gives

$$[R^{**}]_i = \frac{K_1[M]_i[R^*]_i}{K_2 + K_3[M]_i} \quad (i = 1, 2) \quad (18)$$

Substituting equation (18) into equation (14), one obtains

$$[R^{**'}]_i = \frac{K_1K_2[M]_i[R^*]_i}{(K_2 + K_3[M]_i)(K_4[M]_i + K_5)} \quad (i = 1, 2) \quad (19)$$

Substituting equation (19) into equation (10), and keeping in mind that $[R^{*'}]_1 = 0$, one has

$$[Cl^*]_1 = \left[\frac{K_1K_2K_5[M]_1[R^*]_1}{(K_2 + K_3[M]_1)(K_4[M]_1 + K_5)} + K_{de}[Cl^*]_2\right] \Big/ K'_{p1}[M]_1 \quad (20)$$

Reaction (9) is a very active reaction and hence $K'_{p1}[M]_1 \gg K_{de}[Cl^*]_2$ can be assumed. Thus, equation (20) is simplified to

$$[Cl^*]_1 = \frac{K_1K_2K_5[R^*]_1}{K'_{p1}(K_2 + K_3[M]_1)(K_4[M]_1 + K_5)} \quad (21)$$

Similarly, substituting equations (17) and (19) into equation (11), one has

$$[Cl^*]_2 = \frac{K_1K_2K_5[R]^*_2[M]_2}{(K_2 + K_3[M]_2)(K_4[M]_2 + K_5) \times (K'_{p2}[M]_2 + K'_{fp}(Q_1)_2 + K_{de} - K')} \quad (22)$$

where

$$K' = \frac{K_{e2}K'_{fp}(Q_1)_2}{K_{p2}[M]_2 + K_{e2}}$$

From information on microstructure of PVC, one knows that reaction (9) is much faster than reactions (10) and (12). Hence $K'_{p2}[M]_2 \gg K'_{fp}(Q_1)_2$ and $K'_{p2}[M]_2 \gg K_{de}$ can be assumed. $K'$ is very small because $K_{p2} \gg K_eK'_{fp}$. Therefore, $K'_{p2}[M]_2 \gg [K'_{fp}(Q_1)_2 + K_{de} - K']$, and equation (22) can be simplified to

$$[Cl^*]_2 = \frac{K_1K_2K_5[R^*]_2}{K'_{p2}(K_2 + K_3[M]_2)(K_4[M]_2 + K_5)} \quad (23)$$

Comparing reaction (9) with the classical chain transfer to monomer reaction, one finds that the following equation should hold

$$K'_{p1}[Cl^*]_1[M]_1 = (K_{fm})_1[R^*]_1[M]_1 \quad (24)$$

Substituting equation (21) into equation (24), one has

$$(K_{fm})_1 = \frac{K_1K_2K_5}{(K_2 + K_3[M]_1)(K_4[M]_1 + K_5)} \quad (25)$$

Similarly,

$$(K_{fm})_2 = \frac{K_1K_2K_5}{(K_2 + K_3[M]_2)(K_4[M]_2 + K_5)} \quad (26)$$

From equations (25) and (26), one can see that the effective rate constant for chain transfer to monomer is a function of monomer concentration.

Using equations (25) and (26), one may rewrite equations (21) and (23) as

$$[Cl^*]_1 = \frac{(K_{fm})_1}{K'_{p1}}[R^*]_1 \quad (27)$$

$$[Cl^*]_2 = \frac{(K_{fm})_2}{K'_{p2}}[R^*]_2 \quad (28)$$

Using chain transfer to monomer constants reported in the literature, one can estimate that the concentration of chlorine radicals is at least three orders of magnitude smaller than the polymer radical concentration. Therefore, bimolecular termination reactions with Cl· can be neglected.

From equation (15), one has

$$[R^*_i]_j = \frac{R_{Ij}}{K_{ij}[M]_j + K'_{tj}[R^*]_j} \quad (j = 1, 2) \quad (29)$$

The primary radical concentration in equation (29) is also three to four orders of magnitude smaller than the polymer radical concentration. Hence bimolecular termination with $R_i^*$ may not be significant during VCM polymerization.

Substituting equation (28) into equation (9), one can find that

$$[R_1^*]_2 = \frac{R_{I2} + (K_{fm})_2[R^*]_2[M]_2}{K_{p2}[M]_2 + K_{t2}[R^*]_2 + K_{de}} \quad (30)$$

From equation (16), one has

$$[R^*_r]_2 = \left(\frac{1}{\tau}\right)^{r-1}[R^*_1]_2 \quad (31)$$

where

$$\tau = K_{t2}[R^*]_2/K_{p2}[M]_2$$

Substituting equation (30) into equation (31) and considering $K_{p2}[M]_2 \gg K_{t2}[R^*]_2 + K_{de}$ and $R_{I2} \gg (K_{fm})_2[R^*]_2[M]_2'$, one can simplify $[R^*_r]_2$ as

$$[R^*_r]_2 = \left(\frac{1}{\tau}\right)^{r-1}\frac{R_{I2}}{K_{p2}[M]_2} \quad (32)$$

Therefore, the desorption term in equations (7) and (8) can be written as

$$K_{de}\sum_{r=1}^{n}[R^{\bullet}_{r}]_2 = K_{de}\sum_{r=1}^{n}\left(\frac{1}{\tau}\right)^{r-1}\frac{R_{I2}}{K_{p2}[M]_2} = K'_{de}R_{I2} \tag{33}$$

Based on the above discussion and noticing that

$$K'_{p1}[Cl^{\bullet}]_1[M]_1 = K_5[R^{\bullet *\prime}]_1$$

$$K'_{p2}[Cl^{\bullet}]_2[M]_2 + K'_{fp}[Cl^{\bullet}]_2(Q_1)_2 = K_5[R^{\bullet *\prime}]_2$$

equations (7) and (8) can be simplified to

$$\frac{d(R^{\bullet})_1}{V_1\,dt} = R_{I1} - K_{p1}[M]_1[R^{\bullet}_{r_c-1}]_1 - K_{t1}[R^{\bullet}]_1^2 + K'_{de}R_{I2}V_2/V_1 = 0 \tag{34}$$

$$\frac{d(R^{\bullet})_2}{V_2\,dt} = R_{I2} + K_{p1}[M]_1[R^{\bullet}_{r_c-1}]_1V_1/V_2 - K_{t2}[R^{\bullet}]_2^2 - K'_{de}R_{I2} = 0 \tag{35}$$

where $K_{p1}[M]_1[R^{\bullet}_{r_c-1}]_1$ represents the formation and precipitation rate of radicals with chain length $r_c$ in the monomer phase. $[R^{\bullet}_{r_c-1}]_1$ can be obtained by the following equations

$$\frac{dR^{\bullet}_{r-1}}{V_1\,dt} = K_p[R^{\bullet}_{r-2}]_1[M]_1 - K_p[R^{\bullet}_{r-1}]_1[M]_1 - K_{t1}[R^{\bullet}]_1[R^{\bullet}_{r-1}]_1 - K_5[R^{\bullet *\prime}_{r-1}]_1 = 0 \tag{36}$$

$$\frac{dR^{\bullet *}_{r-1}}{V_1\,dt} = K_2[R^{\bullet *}_{r-1}]_1 - K_4[R^{\bullet *\prime}_{r-1}]_1[M]_1 - K_5[R^{\bullet *\prime}_{r-1}]_1 = 0 \tag{37}$$

$$\frac{dR^{\bullet *}_{r-1}}{V_1\,dt} = K_1[R^{\bullet}_{r-2}]_1[M]_1 - K_2[R^{\bullet *}_{r-1}]_1 - K_3[R^{\bullet *}_{r-1}]_1[M]_1 = 0 \tag{38}$$

$$\frac{dR^{\bullet}_{1}}{V_1\,dt} = R_{I1} + K'_p[Cl^{\bullet}]_1[M]_1 - K_p[M]_1[R^{\bullet}_1]_1 - K_{t1}[R^{\bullet}]_1[R^{\bullet}_1]_1 = 0 \tag{39}$$

From equations (36)–(38), one can find

$$[R^{\bullet}_{r-1}]_1 = \frac{K_p[M]_1 - (K_{fm})_1[M]_1}{K_p[M]_1 + K_{t1}[R^{\bullet}]_1}[R^{\bullet}_{r-2}]_1 = \left(\frac{1-C_m}{1+K_{t1}[R^{\bullet}]_1/K_p[M]_1}\right)[R^{\bullet}_{r-2}]_1 = \left(\frac{1-C_m}{1+K_{t1}[R^{\bullet}]_1/K_p[M]_1}\right)^{r-2}[R^{\bullet}_1]_1 = (1-C_m)^{r-2}[R^{\bullet}_1]_1 \tag{40}$$

where $K_{t1}[R^{\bullet}]_1/K_p[M]_1 \ll 1$ is assumed.

Let $r = r_c$. Then equation (40) becomes

$$[R^{\bullet}_{r_c-1}]_1 = (1-C_m)^{r_c-2}[R^{\bullet}_1]_1 \tag{41}$$

where $C_m = (K_{fm})_1/K_p$.

Substituting equation (27) into equation (39) and considering $K_p[M]_1 \gg K_{t1}[R^{\bullet}]_1$, one has

$$[R^{\bullet}_1]_1 = \frac{R_{I1} + (K_{fm})_1[M]_1[R^{\bullet}]_1}{K_{p1}[M]_1} \tag{42}$$

Substituting equation (42) into equation (41), one gets

$$[R^{\bullet}_{r_c-1}]_1 = K^*\frac{R_{I1} + (K_{fm})_1[M]_1[R^{\bullet}]_1}{K_{p1}[M]_1} \tag{43}$$

where

$$K^* = (1-C_m)^{r_c-2}$$

a precipitation constant for polymer radicals.

Substituting equation (43) into equations (34) and (35), one finally obtains the total radical balance for VCM polymerization as follows:

$$R_{I1} - K^*(R_{I1} + (K_{fm})_1[M]_1[R^{\bullet}]_1) - K_{t1}[R^{\bullet}]_1^2 + K'_{de}R_{I2}V_2/V_1 = 0 \tag{44}$$

$$R_{I2} + K^*(R_{I1} + (K_{fm})_1[M]_1[R^{\bullet}]_1)V_1/V_2 - K_{t2}[R^{\bullet}]_2^2 - K'_{de}R_{I2} = 0 \tag{45}$$

Solving equations (44) and (45), one can obtain the polymer radical concentrations for both phases (loci of polymerization) as follows:

$$[R^{\bullet}]_1 = \frac{(J_1^2 + 4K_{t1}J_2)^{1/2} - J_1}{2K_{t1}} \tag{46}$$

$$[R^{\bullet}]_2 = \left\{\frac{R_{I2}(1-K'_{de}) + K^*R_{I1}V_1/V_2 + J_1(V_1/V_2)[(J_1^2 + 4K_{t1}J_2)^{1/2} - J_1]/2K_{t1}}{K_{t2}}\right\}^{1/2} \tag{47}$$

where

$$J_1 = K^*(K_{fm})_1[M]_1$$

$$J_2 = R_{I1}(1-K^*) + K'_{de}R_{I2}V_2/V_1$$

*Monomer concentrations*

During suspension polymerization, monomer partitions in monomer, polymer, water and vapour phases, respectively. Monomer in the water and vapour phases was ignored during kinetic modelling by previous investigators. The total amount of monomer in the water and vapour phases is ≈4% under commercial reactor operation conditions. Hence it is important to consider monomer distribution for valid kinetic/reactor modelling. The monomer distribution as a function of conversion and reactor operation conditions was developed in a previous paper[85]. The main equations are summarized here:

$$M_1 = M_0(1-X) - M_g - M_w - M_2 \tag{48}$$

$$M_g = \frac{M_mP^{\circ}_m}{RT}\left[(1.0 - W_i)V_r + \frac{XM_0(1/D_m - 1/D_p)}{1 - D_{g0}/D_m}\right] \tag{49}$$

$$M_w = KW_w \tag{50}$$

$$M_2 = X[M_0(1-X_f) - M_{gX_f} - M_w]/X_f \tag{51}$$

where

$$M_{gX_f} = \frac{M_mP^{\circ}_m}{RT}\left[(1.0 - W_i)V_r + \frac{X_fM_0(1/D_m - 1/D_p)D_m}{D_m - D_{g0}}\right]$$

If volume additivity is assumed, the volumes of monomer and polymer phase are:

$$V_1 = M_1/D_m \tag{52}$$

$$V_2 = M_2/D_m + M_0X/D_p \tag{53}$$

Hence

$$[M]_1 = D_m/M_m \tag{54}$$

$$[M]_2 = M_2/M_mV_2 \tag{55}$$

*Initiator partition, efficiency and decomposition rate constant*

According to the two-phase polymerization scheme, initiation reactions occur in both monomer and polymer phases. The ratio of initiation rates per unit volume in the monomer and polymer phases can be expressed as a constant because the monomer concentrations in the two phases are constant for the conversion range $X < X_f$, i.e.:

$$K_I = \frac{R_{I2}}{R_{I1}} = \frac{2f_2K_{d2}[I]_2}{2f_1K_{d1}[I]_1} \tag{56}$$

If $K_{d2} = K_{d1}$ and $f_2 = f_1$ are assumed, equation (52) becomes

$$K_I = [I]_2/[I]_1 \tag{57}$$

where $K_I$ is a initiator partition coefficient depending on solubility of the initiator in both monomer and polymer phases. However, solubility data for initiator in monomer and polymer phases are not available. Therefore, $K_I$ is used as an adjustable parameter in the model. Based on a total initiator mole balance, the initiator concentrations can be written as:

$$[I]_1 = I_0 \exp(-K_dt)/(V_1 + K_IV_2) \quad (\text{mol l}^{-1}) \tag{58}$$

$$[I]_2 = K_I[I]_1 \quad (\text{mol l}^{-1}) \tag{59}$$

Decomposition rate constants and efficiencies of initiators depend on solvent type as well as temperature. The initiation mechanism can be expressed as follows:

| | | |
|---|---|---|
| (a) | $I \xrightarrow{K_d} 2[R_i^{\bullet}]$ | radical pair in cage |
| (b) | $2[R_i^{\bullet}] \xrightarrow{K_{R1}}$ inert | recombination in cage |
| (c) | $2[R_i^{\bullet}] \xrightarrow{K_{R2}}$ I (peroxide) | recombination in cage |
| (d) | $2[R_i^{\bullet}] \xrightarrow{K_D} 2R_i^{\bullet}$ | diffusion out of cage |
| (e) | $2[R_i^{\bullet}] \xrightarrow{K_x} R_1^{\bullet} + R_i^{\bullet}$ | reaction of radical pair with monomer |
| (f) | $R_i^{\bullet} + M \xrightarrow{K_p} R_1^{\bullet}$ | generation of polymer radical chain length unity |

Based on the definition of initiator efficiency and use of the stationary-state hypothesis, one can find

$$f = \frac{K_D + K_x[M]}{K_{R1} + K_D + K_x[M]} \tag{60}$$

For peroxide initiators, reaction (b) may involve decarboxylation and $\beta$ scission reactions. If $K_{R2} \gg K_{R1}$, reaction (b) can be neglected and initiator efficiency of peroxide initiators can then be simplified to:

$$f \approx 1 \quad \text{(peroxide initiator)} \tag{61}$$

Therefore, for the azo initiator system, $f$ is a function of conversion. For certain peroxide initiator systems, the initiator efficiency is equal to or close to one, but the decomposition rate of initiator is governed by reactions (a) and (c), i.e.:

$$-\frac{d[I]}{dt} = K_d[I] - K_{R2}[2R_i^{\bullet}]$$

$$= K_d\left(\frac{K_{R2} + K_D + K_x[M]}{K_{R1} + K_{R2} + K_D + K_x[M]}\right)[I]$$

$$= K_d'[I] \tag{62}$$

where

$$K_d' = K_d\frac{K_{R2} + K_D + K_x[M]}{K_{R1} + K_{R2} + K_D + K_x[M]}$$

an effective decomposition rate constant.

From equation (62), one can see that the analysis of concentration of initiator in a solvent gives the effective decomposition rate constant $K_d'$ instead of $K_d$. This may partly explain why the decomposition rate constant of peroxide initiators depends on solvent type. Hence the effective decomposition rate constant of the peroxide is a function of conversion at high conversions.

Using radical and monomer concentrations and initiator partition coefficient, one can express polymerization rate as a function of the physical properties of the reaction system and reactor operation conditions. Substituting equation (46) and (47) into (6), one can rewrite the polymerization rate as

$$\frac{dX}{dt} = \frac{1}{N_0M_m}\Bigg\langle K_{p1}[(J_1^2 + 4K_{t1}R_{I1}J_2)^{1/2} - J_1]M_1/2K_{t1}$$

$$+ \frac{K_{p2}}{K_{t2}^{1/2}}\Bigg\{R_{I2}(1 - K_{de}') + K^*R_{I1}V_1/V_2$$

$$+ \frac{J_1V_1}{2K_{t1}V_2}[(J_1^2 + K_{t1}J_2)^{1/2} - J_1]\Bigg\}^{1/2}M_2\Bigg\rangle \tag{63}$$

where $M_1$ and $M_2$ are shown as equations (48)–(51).

Equation (63) describes the total polymerization rate of VCM in two phases. This model shows that the Talamini model is a special case of the present model.

If $K^* = 0$ and $K_{de}' = 0$, equation (63) gives:

$$\frac{dX}{dt} = \frac{1}{N_0M_m}\left(\frac{K_{p1}}{K_{t1}^{1/2}}R_{I1}^{1/2}M_1 + \frac{K_{p2}}{K_{t2}^{1/2}}R_{I2}^{1/2}M_2\right) \tag{64}$$

Equation (64) indicates that the polymerization occurs in two phases independently. This equation will lead to Talamini's model. $K^* = (1 - C_m)^{r_c - 2} = 0$ means that $r_c = \infty$. Hence precipitation of radicals does not occur during polymerization, which is also the main limitation of Talamini's model.

If $K^* = 1.0$ and $K_{de}' = 0$, equation (63) becomes:

$$\frac{dX}{dt} = \frac{K_{p2}}{N_0M_mK_{t2}^{1/2}}(R_{I2} + R_{I1}V_1/V_2)^{1/2}M \tag{65}$$

which means that all of the polymerization occurs in the polymer phase.

$K^* = 1.0$ is consistent with $r_c = 2$, i.e. the critical chain length for precipitation is two monomeric units. All the radicals will precipitate and transfer to the polymer phase before further propagation and termination occurs in the monomer phase.

Therefore, $K^*$ must be between 0 and 1 ($0 < K^* < 1$). The value of $K^*$ observed will show how significant the precipitation of radicals is during polymerization.

When $X > X_f$, the monomer phase no longer exists and the polymerization proceeds in the polymer phase. In fact, the expressions for radical and monomer concentrations in this conversion range are straightforward. However, the kinetic rates which become diffusion-controlled will have associated rate constants which depend on polymer concentration and thus on monomer conversion. The modelling of diffusion-controlled reactions will be discussed later. The polymerization rate can now be expressed in the usual form as

$$\frac{dX}{dt} = \frac{K_{p2}}{N_0 M_m} (R_{12}/K_{t2})^{\frac{1}{2}} M_2 \tag{66}$$

where

$$M_2 = M_0(1 - X) - M_g - M_w$$

$$M_g = \frac{M_m P_m}{RT}\left[(1.0 - W_i)V_r + M_0(1/D_m - 1/D_p) \times \left(X + X_f \frac{D_{g0}}{D_m - D_{g0}}\right)\right]$$

$$M_w = K W_w P_m / P_m^\circ$$

$$R_{12} = 2fK_d I_0 \exp(-K_d t)/V_2$$

*Limiting conversion*

The glassy-state transition temperature of commercial PVC is about 80°C, which is higher than the normal polymerization temperatures used. The glassy-state transition temperatures of PVC–VCM mixtures (the monomer acting as a plasticizer) are lower than that of pure PVC. Therefore, for the commercial polymerization temperature range, PVC–VCM mixtures (polymer phase) will experience a glassy-state transition below 100% monomer conversion. The conversion at which the polymer phase experiences a glassy-state transition is called the limiting conversion. Polymerization now occurs in the solid state with rates that for production purposes may be considered zero. The limiting conversion $X_L$ may be expressed as

$$X_L = \frac{M_0 - M_2 - M_w - M_g}{M_0} \tag{67}$$

where

$$M_2 = \frac{M_0 X_L D_m (1 - \phi_p)}{D_p \phi_p} \tag{68}$$

$$M_w = K W_w P_m / P_m^\circ \tag{69}$$

$$M_g = \frac{M_m P_m}{RT}\left[(1 - W_i)V_r + M_0(1/D_m - 1/D_p)\left(X_L + X_f \frac{D_{g0}}{D_m - D_{g0}}\right)\right] \tag{70}$$

Substituting equations (68)–(70) into equation (67), one has

$$X_L = \frac{M_0 - K W_w P_m / P_m^\circ - M'_{gX_f}}{M_0\{1 + [D_m(1 - \phi_p)/D_p\phi_p] + M_m P_m (1/D_m - 1/D_p)/RT\}} \tag{71}$$

where

$$M'_{gX_f} = \frac{M_m P_m}{RT}\left[(1 - W_i)V_r + \frac{X_f M_0 (1/D_m - 1/D_p) D_{g0}}{D_m - D_{g0}}\right]$$

According to the free volume theory[92], the free volume fraction of the polymer–monomer mixture may be expressed as:

$$V_f = [0.025 + \alpha_p(T - T_{gp})]\phi_p + [0.025 + \alpha_m(T - T_{gm})](1 - \phi_p) \tag{72}$$

At the glassy-state transition, the free volume fraction is taken to be 0.025. Hence, polymer volume fraction at the glassy transition state can be expressed as:

$$\phi_p = \frac{\alpha_m(T - T_{gm})}{\alpha_p(T_{gp} - T) + \alpha_m(T - T_{gm})} \quad (T_{gm} < T < T_{gp}) \tag{73}$$

Partial pressure of monomer can be calculated using the Flory–Huggins equation[93]:

$$P_m / P_m^\circ = (1 - \phi_p)\exp(\phi_p + \chi\phi_p^2) \tag{74}$$

Substituting equations (73) and (74) into equation (71), one can find the limiting conversion as a function of reactor operation conditions and the physical properties of polymer phase.

*Diffusion controlled reactions in the polymer phase*

Several attempts have been made to model diffusion-controlled termination and propagation[17,90]. However, the fall in initiator efficiency at high conversions has been neglected. Hamielec *et al.*[90] first applied the free-volume theory to model diffusion-controlled termination and propagation to explain the properties of PVC obtained at high monomer conversions. These modelling attempts were premature due to the inadequate amount of kinetic data at these high conversion levels.

The free radical polymerization of VCM involves four reaction types based on the size of the reactants:

(1) single molecules, such as reactions (1), (5), (8), (12) and (19);

(2) two small molecules, such as reactions (2) and (9);

(3) macromolecule and a small molecule, such as reactions (3), (4), (6), (7), (10), (11), (14), (20); and

(4) two macromolecules, such as reactions (13), (15) and (16).

These reactions occur in both monomer and polymer phase simultaneously. The monomer phase is essentially pure monomer due to the low solubility of PVC. Hence, all the reactions in the monomer phase are probably chemically controlled. However, the polymer phase contains $\approx 70$ wt% polymer over the conversion range, 0 to $X_f$. Therefore, bimolecular termination reactions involving macromolecule reactants should be diffusion controlled in the polymer phase over the entire monomer conversion range. At some conversion, $X > X_f$, it is expected that propagation reactions are diffusion controlled and that the initiator efficiency or decomposition constant falls significantly with conversion.

At glassy-state transition, the propagation reaction rate should fall effectively to zero. The effect of environment on the initiation rate depends on the chemistry of the initiator as mentioned above. For azo initiators, the efficiency will decrease significantly with conversion because $K_D$ would fall appreciably with increase in viscosity of the medium. For peroxide initiators, the

effective decomposition rate constant will decrease significantly with conversion, which has been shown with the experimental results of Marinin *et al.*[19]

Kinetic parameters for diffusion controlled reactions for VCM polymerization are not available in the literature. In the present model, all of the rate constants for diffusion-controlled reactions are modelled using the free volume theory as follows:

$$K_{t2} = K_{t1} \exp\left[ -A^*\left(\frac{1}{V_{fp}} - \frac{1}{V_{fcri}}\right)\right] \quad (75)$$

where $K_{t1}$ and $K_{t2}$ are number-average termination constants (this accounts for chain length dependence of bimolecular termination).

$$K_p = K_{pX_f} \exp\left[ -B^*\left(\frac{1}{V_{fp}} - \frac{1}{V_{fX_f}}\right)\right] \quad (X > X_f) \quad (76)$$

$$K_p f^{1/2} = (K_p f^{1/2})_{xf} \exp\left[ -B_f^*\left(\frac{1}{V_{fp}} - \frac{1}{V_{fX_f}}\right)\right] \quad (X > X_f) \quad (77)$$

$$K_d = K_{dX_f} \exp\left[ -C^*\left(\frac{1}{V_{fp}} - \frac{1}{V_{fX_f}}\right)\right] \quad (X > X_f) \quad (78)$$

where $A^*$, $B^*$, $B_f^*$ and $C^*$ can be estimated by fitting model predictions with experimental rate data. $K_p$ and $f$ cannot be separated for an azo initiator in the present model.

## EXPERIMENTAL

To estimate parameters for the present model, a series of kinetic experiments was made over a wide temperature range.

The equipment used for the experiments included an agitated 5 l stainless steel reactor with a calibrated vacuum pressure gauge and a thermocouple, and a Hewlett Packard (5880 A) gas chromatograph with an automatic gas sampler controlled by a microcomputer. The reactor temperature was maintained by a steam and water mixture that circulated in the reactor jacket, which was controlled by a P.I.D. controller.

The reactor was filled with a weighed amount of deionized, distilled water with dissolved stabilizer and a weighed amount of initiator at a temperature around 10°C. A weighed amount of VCM was injected into the reactor after the reactor was evacuated. The reactor temperature was then raised to the polymerization temperature in ≈5 min. Conversions were determined by the n-butane tracer method which has been discussed in detail in a previous paper[94].

VCM was provided by the B.F. Goodrich Company (Niagara Falls, Ontario, Canada).

Stabilizer, polyvinylalcohol (PK-08) (degree of hydrolysis 71–75 mol%), and initiator, bis(4-tert-butylcyclohexyl) peroxydicarbonate (Perkadox 16-W40) (40% liquid suspension), were provided by AKZO Chemicals (The Netherlands). Azobis(isobutyronitrile) (AIBN) recrystallized was also used as an initiator for polymerizations at higher temperature.

The suspension polymerization conditions and the basic recipe are as follows:

| | |
|---|---|
| reactor volume: | 5.0 l; |
| temperature range: | 40–80°C; |
| monomer: | 1116 g; |
| water: | 2232 g; |
| stabilizer: | 0.08 wt% (based on water); |
| initiator: | various amounts. |

## RESULTS AND DISCUSSION

The present experimental results are shown in *Figures 4–7*. The accuracy of the experimental results was discussed in a previous paper[94].

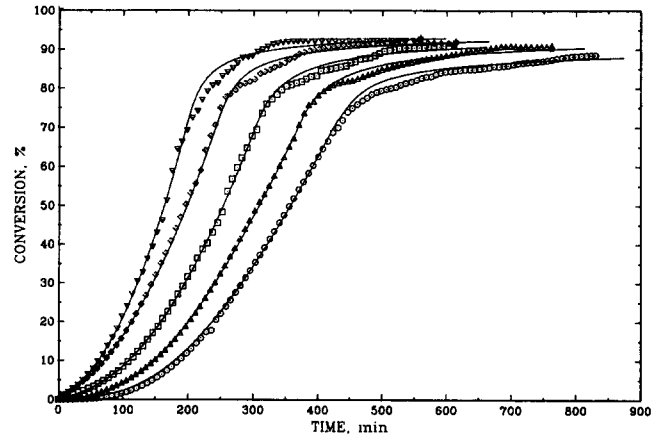


**Figure 4** Conversions *versus* reaction time for suspension polymerization of vinyl chloride at 50°C with Perkadox 16-W40 as initiator. [I] (wt%): ○, 0.100; △, 0.125; □, 0.150; ◇, 0.175; ▽, 0.200; *, Gravimetry; ———, model

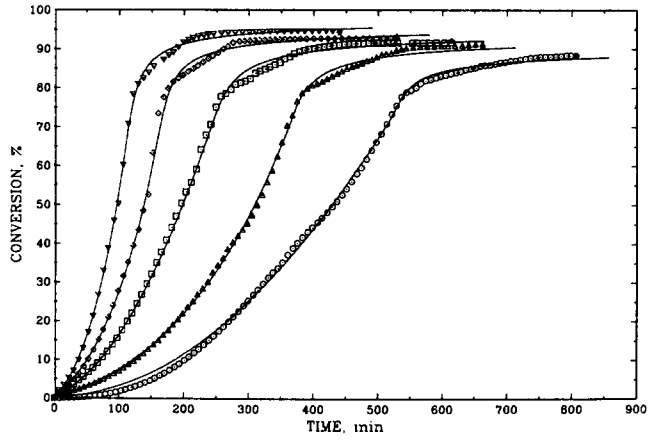


**Figure 5** Suspension polymerization of VCM at different temperatures with Perkadox 16-W40 as initiator, [I] = 0.175 wt%: ○, 40; △, 45; □, 50; ◇, 55; ▽, 60°C; *, gravimetry; ———, model

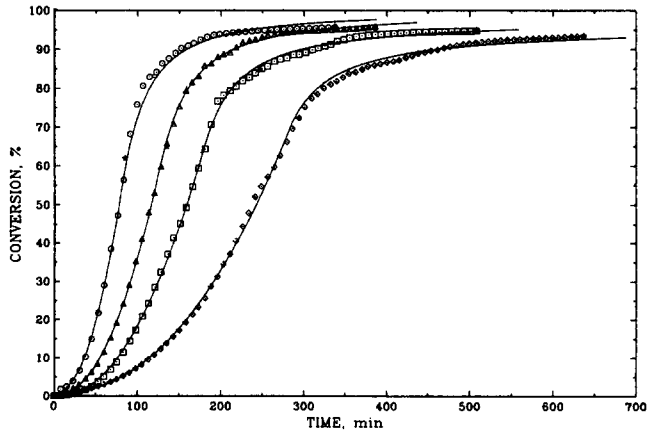


**Figure 6** Suspension polymerization of VCM at different temperatures with AIBN as initiator, [I] = 0.25 wt%: ○, 70; △, 65; □, 60; ◇, 55°C; *, gravimetry; ———, model

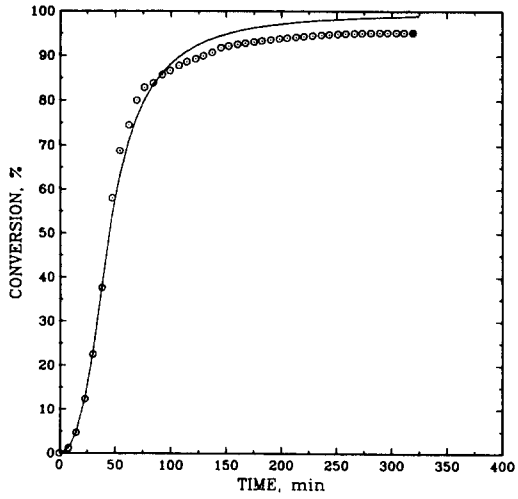


**Figure 7** Suspension polymerization of VCM at 80°C with AIBN as initiator, [I] = 0.15 wt%: ○, experimental data; ———, model

*Physical properties used in the model*

The parameters of physical properties of VCM, water and PVC are as follows[85]:

$$D_m = 947.1 - 1.746t - 3.24 \times 10^3 t^2 \quad (g\,l^{-1}) \quad (79)$$

$$D_p = 10^3 \exp(0.4296 - 3.274 \times 10^{-4} T) \quad (g\,l^{-1}) \quad (80)$$

$$D_w = 1011.0 - 0.4484t \quad (g\,l^{-1}) \quad (81)$$

$$K = 0.0472 - 11.6/T \quad (82)$$

$$P_m^\circ = 12722 \exp(-2411.7/T) \quad (atm) \quad (83)$$

$$\chi = 1286.4/T - 3.02 \quad (84)$$

where $t$ is temperature in °C and $T$ is temperature in K.

The glassy state transition temperature of VCM, $T_{gm}$, was estimated using Fedors universal correlation[95]:

$$T_{gm} = 70.0\ K \quad (85)$$

The glassy state transition temperature of PVC, $T_{gp}$, depends on the synthesis temperature according to the results of Reding *et al.*[96] and Ceccorulli *et al.*[97], as shown in *Figure 8*. The correlation between $T_{gp}$ and polymerization temperature can be obtained using a least squares fit:

$$T_{gp} = 87.1 - 0.132t \quad (86)$$

The glassy state transition temperature of PVC–VCM mixtures as reported in the literature[98–100] are shown in *Figure 9* together with the present limiting conversion data. Fitting equation (73) with these data, one can estimate the thermal expansion factors for VCM and PVC as follows:

$$\alpha_m = 9.98 \times 10^{-4} \quad (87)$$

$$\alpha_p = 5.47 \times 10^{-4} \quad (88)$$

These values are used in the model.

*Kinetic parameters*

The decomposition rate constant of AIBN has been estimated by many investigators[101–106] for different solvents over a wide temperature range. These data are shown in *Figure 10*. One can see that $K_d$ for AIBN is independent of solvent type and level. The temperature dependence of $K_d$ can be estimated using a least squares fit as:

$$K_d = 2.88 \times 10^{15} \exp(-31.2\ kcal/RT) \quad (s^{-1}) \quad (89)$$

The decomposition of Perkadox 16-W40 has not been studied in detail although it is a common initiator in commercial processes. Very limited data have been reported by AKZO chemicals[107] as shown in *Figure 10*. Temperature dependence of $K'_d$ of Perkadox 16-W40 can be estimated roughly as:

$$K'_d = 2.31 \times 10^{15} \exp(-29.1\ kcal/RT) \quad (s^{-1}) \quad (90)$$

Equation (90) can only be used for $X < X_f$. When $X > X_f$, $K'_d$ can be calculated by using equation (78).

The efficiency of AIBN in VCM bulk or suspension polymerization has not been determined. A value of 0.77 was determined by Arnett *et al.*[108] in solution polymerization of VCM and this value will be used in the present model for $X < X_f$. For $X > X_f$, efficiency will be estimated based on equation (77) together with $K_p$.

Individual kinetic constants such as $K_p$ and $K_t$ for bulk or suspension polymerization of VCM are not available in the literature. Normally, the ratio $K_p/K_t^{1/2}$ is estimated based on conversion–time data[13,14,109,110]. However, the results strongly depend on model applied and conversion range used. In the present work, $K_p/K_t^{1/2}$ was estimated by using very low conversion data. At very low conversion, $K^* = 0$, $K'_{de} = 0$ and $M_2 = 0$ may be assumed. Equation (63) can then be simplified for homogeneous polymerization,which can be integrated as

$$-\ln(1 - X) = K_p \left(\frac{2fK_d}{K_t}\right)^{1/2} [I]_0^{1/2} t \quad (91)$$

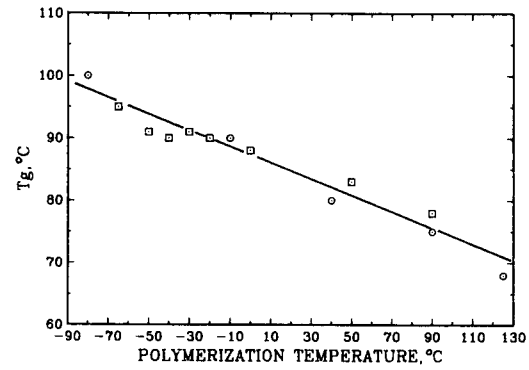


**Figure 8** Polymerization temperature dependence of glassy transition temperature of PVC: ○, Reference 96; □, Reference 97

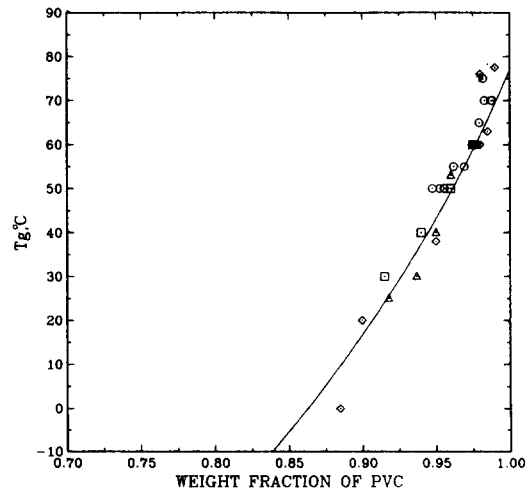


**Figure 9** Glassy transition temperature of PVC–VCM mixture *versus* weight fraction of PVC: ○, present work; △, Reference 98; □, Reference 99; ◇, Reference 100; ———, equation (67)

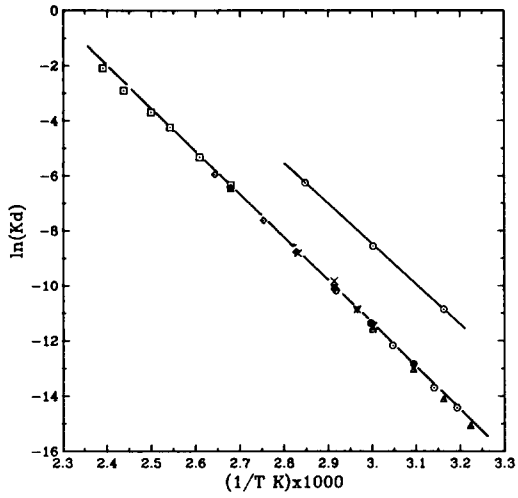


**Figure 10** Decomposition rate constants of AIBN and Perkadox 16-W40: ○ (lower curve), AIBN in benzene[101]; △, AIBN in benzene or toluene[102]; □, AIBN in di-n-butylphthalate[103]; ◇, AIBN in toluene[104]; ×, AIBN in toluene[105]; ▽, AIBN in vinyl chloride monomer[106]; ○, (upper curve), Perkadox 16-W40 in chlorobenzene[107]

Therefore, the initial slope can be found by plotting $-\ln(1-X)$ against $t$ as shown in *Figure 11*. $K_p/K_t^{1/2}$ can be obtained from these initial slopes as shown in *Figure 12*. The relationship between $K_p/K_t^{1/2}$ and temperature was estimated by the least squares method as

$$K_p/K_t^{1/2} = 10.4 \exp(-3.78 \text{ kcal}/RT) \quad (\text{l mol}^{-1}\,\text{s}^{-1}) \tag{92}$$

These results are in agreement with data estimated by Kuchanov *et al.*[14]. The rate constant ratio given by equation (92) was used for polymerization in the monomer phase.

During model evaluation, a group of kinetic constants $(K_{fm})_1/K_{t1}$ is involved, which strongly correlates with other parameters in non-linear regression calculations. Hence the literature values determined in solution polymerization[111] were used in the present model:

$$(K_{fm})_1 = 1.9 \times 10^5 \exp(-7800/RT) \quad (\text{l mol}^{-1}\,\text{s}^{-1})^{\frac{1}{2}} \tag{93}$$

$$K_{t1} = 1.3 \times 10^{12} \exp(-4200/RT) \quad (\text{l mol}^{-1}\,\text{s}^{-1}) \tag{94}$$

The calculation of the critical conversion $X_f$ at which the monomer phase is consumed by the model was illustrated in a previous paper[85]. The critical free volume fraction $V_{fX_f}$ can be calculated by using $X_f$. The critical free volume fraction $V_{fcri}$ at which the bimolecular termination reaction of polymer phase becomes diffusion controlled is difficult to estimate. However, the following inequality should be true:

$$V_{fp} < V_{fcri} < V_{fm} \tag{95}$$

Both $V_{fp}$ and $V_{fm}$ are constant for $X < X_f$. Considering a hypothetical homogeneous PVC–VCM solution, one may assume that the bimolecular termination reaction of polymer radicals becomes diffusion controlled at $\approx 30\%$ conversion. At this conversion for the hypothetical system, $V_{fcri}$ is equivalent to 80% $V_{fm}$. A value of 80% $V_{fm}$ was used for $V_{fcri}$ in the present model.

Desorption of polymer radicals from the polymer phase into the monomer phase involves their molecular diffusion out of primary particles. The desorption rate constant, therefore, is a function of molecular diffusion coefficients and diameter of the primary particle. Applying Nomura's equation[112], one may write the modified desorption rate constant as

$$K'_{de} = K^*_{de}/d_p^2 \tag{96}$$

where $K^*_{de}$ is a function of temperature and $d_p$ is the diameter of the primary particle, which is a function of conversion and temperature.

Information about diameter of primary particle as a function of conversion and temperature is very limited in the literature. Smallwood[66] determined the diameter of primary particles as a function of conversion over the temperature range 51–71°C. Based on Smallwood's data, the diameter of primary particles can be expressed as the following correlation:

$$d_p = [(0.045t(^\circ\text{C}) - 0.76)X^{1/2} - 0.21]10^{-5} \quad (\text{dm}) \qquad (0.02 < X < X_f) \tag{97}$$

The remaining parameters in the present model were estimated with a non-linear regression method, fitting the experimental data with solutions of the differential equation. The results are shown in *Figures 4–6*. One can see that the present model can satisfactorily fit the experimental data over the entire conversion range.

The parameters $K^*$, $A^*$, $K^*_{de}$ and $K_1$ were estimated by using conversion–time data for $X < X_f$. The parameters $B^*$, $B^*_f$, and $C^*$ were estimated by using

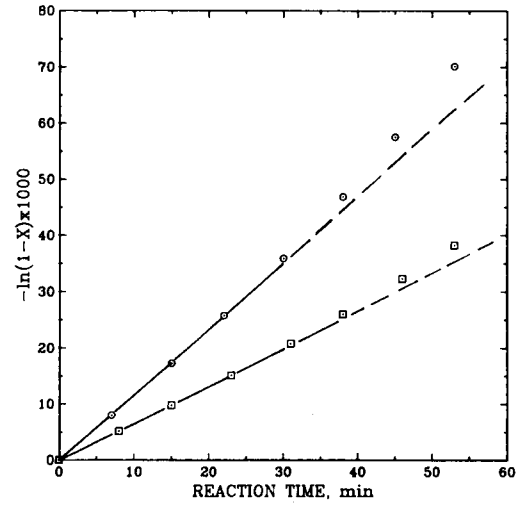


**Figure 11** $-\ln(1-X)$ *versus* reaction time for VCM suspension polymerization at 50°C: ○, Perkadox 16-W40; □, AIBN

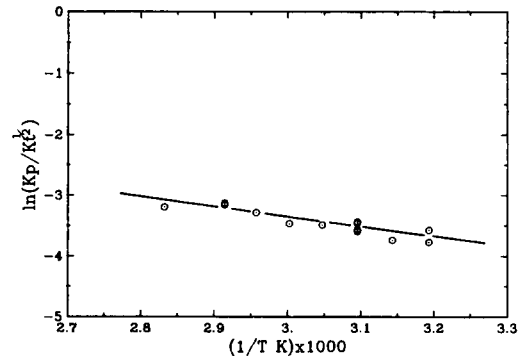


**Figure 12** $K_p/K_t^{1/2}$ *versus* reaction temperature for VCM polymerization at low conversion

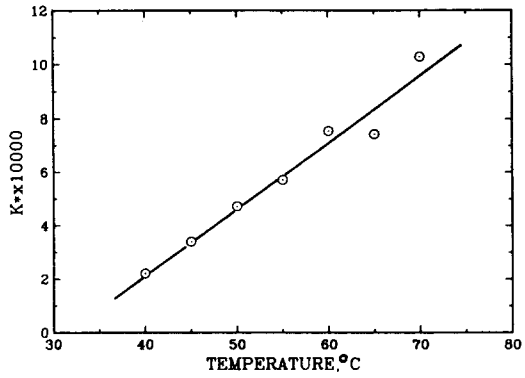


**Figure 13** Temperature dependence of $K^*$

conversion–time data for $X > X_f$. The results are shown in *Figures 13* and *15–17*.

In *Figure 13*, one can see that $K^*$ increases with polymerization temperature. The temperature dependence of $K^*$ can be expressed using the following correlation:

$$K^* = [0.25t(°C) - 7.89] \times 10^{-4} \quad (98)$$

With $K^*$ values, one can estimate the significance of the precipitation of radicals from the monomer phase. At 50°C, for example, $K^* \approx 4.7 \times 10^{-4}$, which indicates that $\approx 4.7 \times 10^{-2}\%$ radicals produced from initiation and transfer to monomer will precipitate out from the monomer phase before termination based on the present model equations (44) and (45). This magnitude of $K^*$ indicates that the precipitation may not affect the radical concentration in the monomer phase significantly. However, the precipitation of these radicals will increase the radical concentration in the polymer phase significantly at relatively low conversion, because the ratio of reaction volume between monomer and polymer phase is very high at low conversions as shown in *Figure 14*. This effect will decay dramatically with conversion. $K^*$ estimated in the kinetic model is based on radical population in the different phases. It may not give accurately the thermodynamic solubility chain length.

Temperature dependence of $K^*_{de}$ is shown in *Figure 15*. It can be expressed as the following correlation:

$$K^*_{de} = 5.08 \times 10^{-8} \exp(-4790/T) \quad (dm^2) \quad (99)$$

Substituting equations (97) and (99) into equation (96), one can find $K'_{de}$. At 50°C, for example, $K'_{de} \approx 0.5$ when the diameter of PVC particles is $\approx 0.02\ \mu m$ at $\approx 2\%$ conversion. The desorption of radicals from the polymer phase is very significant at this stage. However, when the diameter of the primary particles is $\approx 0.5\ \mu m$ at $\approx 20\%$ conversion, $K'_{de}$ is as small as 0.0008. Therefore, the desorption of radicals is negligible when the diameter of primary particles is $> 0.5\ \mu m$. Although desorption of radicals is very significant at low conversion, it will not affect radical concentration in the monomer phase because the volume of polymer phase is very small compared with that in the monomer phase. With $K^*$ and $K'_{de}$ values, one can conclude that the absorption and desorption of radicals are significant only at very low conversions ($< 10\%$ conversion). Radical exchange between phases only affects radical concentration in the polymer phase. This effect cannot even dominate the radical concentrations in both phases at very low conversions.

Initiator partition coefficients have been neither independently measured experimentally nor estimated by modelling. It has often been assumed that $K_I \leqslant 1$ in the literature[16,17]. This study is the first time that $K_I$ has been estimated by fitting a model with conversion–time data. One can see, from *Figure 16*, that $K_I$ values are very scattered and seem to be independent of temperature and initiator type. The average $K_I$ value is 0.77 based on the present data. Note that $K^*$ and $K_I$ are highly correlated in the present estimation. Therefore, it is difficult to estimate these values precisely. However, it appears that $K_I < 1$.

*Figure 17* shows the temperature dependence of the free volume parameters. The correlations obtained by least squares fitting are as follows

$$A^* = 6.64 \times 10^6 \exp(-4986/T) \quad (100)$$

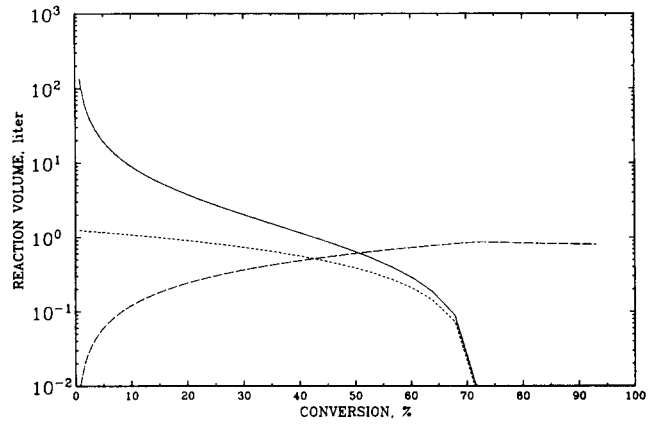


**Figure 14** Reaction volume and the ratio of reaction volume *versus* conversion at 50°C: ———, reaction volume in the monomer phase; – – –, reaction volume in the polymer phase; ———, the ratio of reaction volume, $V_1/V_2$

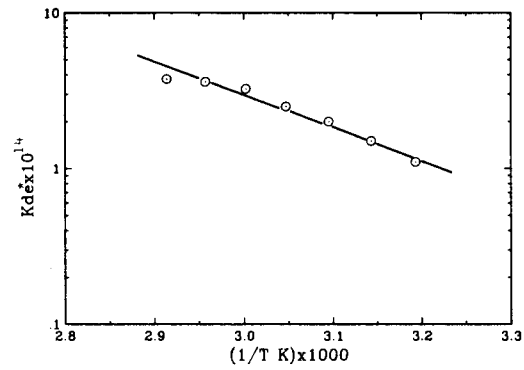


**Figure 15** Temperature dependence of $K^*_{de}$

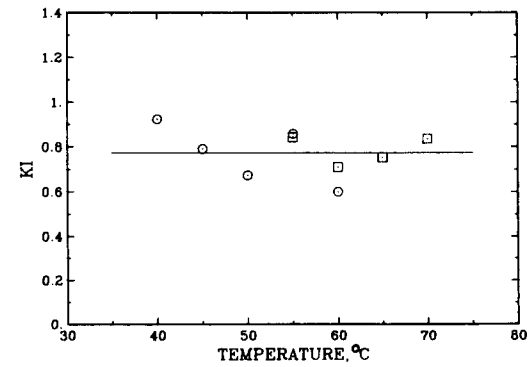


**Figure 16** Initiator partition coefficient

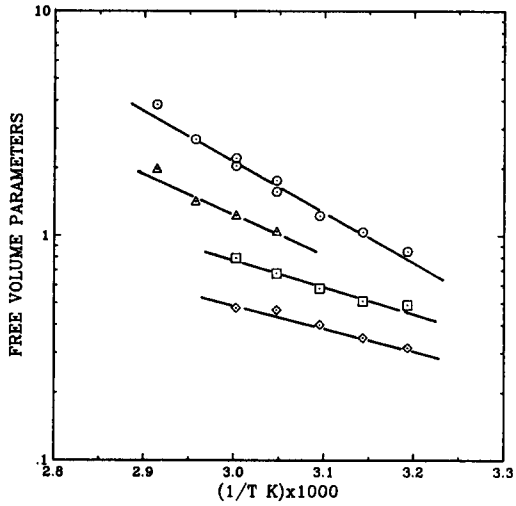


**Figure 17** Temperature dependence of free volume parameters: ○, $A^*$; △, $B_f^*$; □, $B^*$; ◇, $C^*$

$$B^* = 1.85 \times 10^3 \exp(-2595/T) \quad (101)$$

$$B_f^* = 4.01 \times 10^4 \exp(-3464/T) \quad (102)$$

$$C^* = 477.0 \exp(-2291/T) \quad (103)$$

From equations (100)–(103), one can see that $A^* > B^* > C^*$ at a given temperature. These values imply that the sensitivity of bimolecular termination, propagation and initiation to change in free volume at high conversion also follows this order.

All the parameters involved in the model have been estimated as discussed above. With these parameters, one can further predict the features of VCM polymerization quantitatively.

*Simulations using the present model*

With the physical and kinetic parameters estimated above, one can quantitatively describe the features of the two-phase polymerization of VCM.

*Figure 18* shows the monomer distribution during suspension polymerization under the present experimental conditions. The total amount of monomer in the monomer phase decreases gradually with conversion until $X_f$, at which time the free monomer is consumed. For $X > X_f$, monomer concentration in the polymer phase decreases gradually with time until the limiting conversion $X_L$ is reached. A total of $\approx 4\%$ of monomer is in the water and gas phases.

*Figure 19* shows the partition of initiator between the two phases. Initiator concentrations in both monomer and polymer phases increase significantly for AIBN. Therefore, the total concentration of AIBN increases with conversion before $X_f$. This is because the decomposition rate of AIBN is very small and the reaction volume shrinks, the consequence being an increase of total concentration of AIBN. At very high conversions, the reaction rate is very slow. Hence reaction volume shrinkage rate is also very slow, but the decomposition of AIBN still proceeds and the total concentration of AIBN decreases as a result. For Perkadox 16-W40, the total concentration of initiator decreases gradually because the decomposition rate of Perkadox 16-W40 is much higher than the reaction volume shrinking rate before $X_f$. At high conversions, the concentration of initiator increases slightly because of the decrease of $K_d'$ and reaction volume.

Equation (5) shows that, in general, the radical concentration in the polymer phase is higher than that in the monomer phase. Based on the present model predictions, as shown in *Figure 20*, radical concentration in the polymer phase is about 30 times that in the monomer phase at 50°C. This is the consequence of the lower termination rate in the polymer phase. It also explains the auto-acceleration in polymerization rate observed for VCM polymerization. At high conversions, the radical concentration increases dramatically. The model prediction of radical concentration needs to be tested by radical concentration measurements.

If $K_{t1}$ in equation (94) is used for the monomer phase, the polymerization rates in the monomer and polymer phases can be calculated, respectively, as shown in *Figure 21* together with the total polymerization rate. In *Figure 21*, one can see that the reaction rate in the monomer

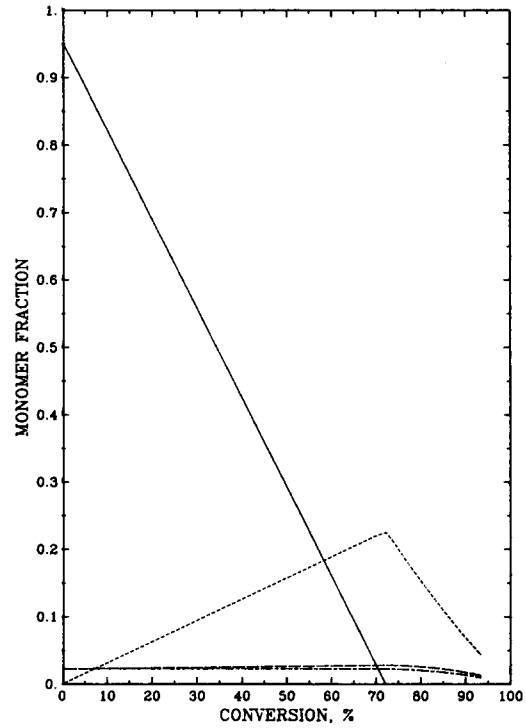


**Figure 18** Monomer distribution of suspension polymerization of vinyl chloride at 50°C: ———, monomer phase; - - - - -, polymer phase; ———, gas phase; - - - - -, water phase

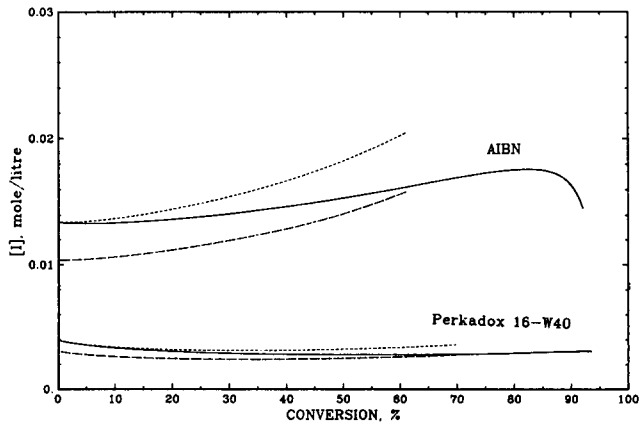


**Figure 19** Initiator concentration *versus* conversion for suspension polymerization of VCM: - - - - -, monomer phase; ———, polymer phase; ———, total concentration of initiator

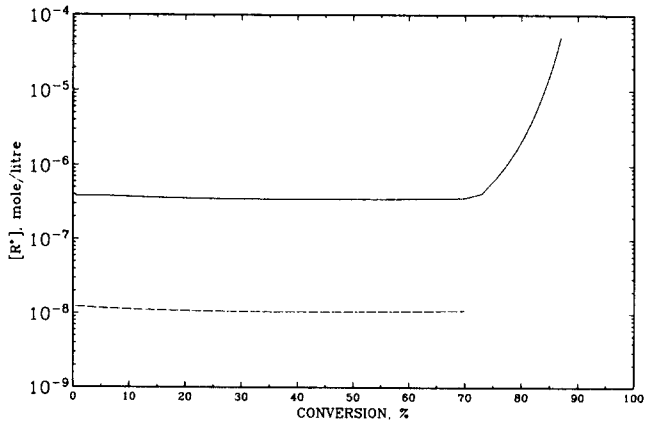


**Figure 20** Radical concentrations in two phases at 50°C with Perkadox 16-W40 as initiator, [I] = 0.175 wt%: ———, polymer phase; ----, monomer phase

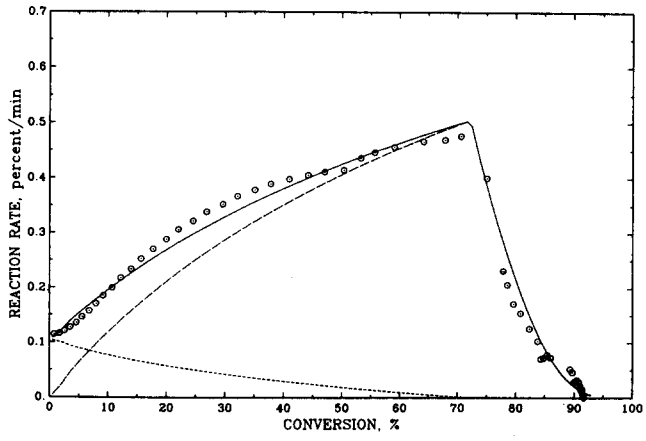


**Figure 21** Polymerization rate *versus* conversion in different phases with Perkadox 16-W40 as initiator, [I] = 0.175 wt%, present experimental data; -----, monomer phase; ----, polymer phase; ———, total polymerization rate

phase gradually decreases with conversion and the reaction rate in the polymer phase increases dramatically with conversion until $X_f$, and then decreases sharply until limiting conversion $X_L$. The monomer phase dominates the polymerization rate only below $\approx 7\%$ conversion at 50°C. At higher conversions polymerization in the polymer phase dominates. This is in agreement with the assumption of several previous investigators[12,15,82]. The total polymerization rate is in excellent agreement with the experimental rate data calculated by differentiating conversion–time data, as shown in *Figure 22*. The highest reaction rate occurs at a conversion near $X_f$.

*Figures 4–7, 18* and *22* all show that the polymerization rate falls dramatically beyond conversion $X_f$. *Figures 23–26* further show the change of model parameters. Beyond $X_f$, the monomer phase does not exist and polymerization continues in the primary particles and their agglomerates. Hence, the free volume fraction decreases gradually with conversion until the glassy state transition as shown in *Figure 23*. With decreasing free volume, the termination and propagation rate constants and initiator efficiency for AIBN and decomposition rate constant for peroxide decrease dramatically. The rate of change depends on the nature of the reactions, as shown in *Figures 24–26*.

The limiting conversion varies with polymerization temperature as shown in *Figure 27*. The experimental data are the final conversions obtained by the present experiments. The difference between predicted limiting conversion and experimental data is $< 1\%$. The polymerization times in our experiments are much longer than typical commercial polymerization times. Hence *Figure 27* also suggests that the limiting conversion cannot be reached with commercial polymerization times. Theoretically, 100% conversion can be reached if the polymerization temperature is higher than the glassy state transition

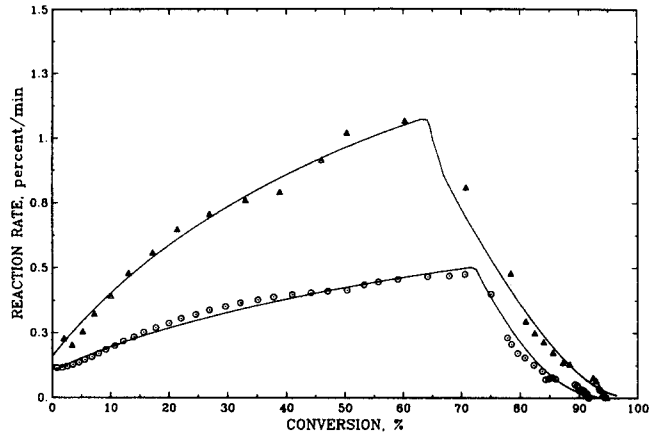


**Figure 22** Total polymerization rate *versus* conversion at different temperature with Perkadox-16 as initiator, [I] = 0.175 wt%: Δ, 60°C; ○, 50°C; ———, model

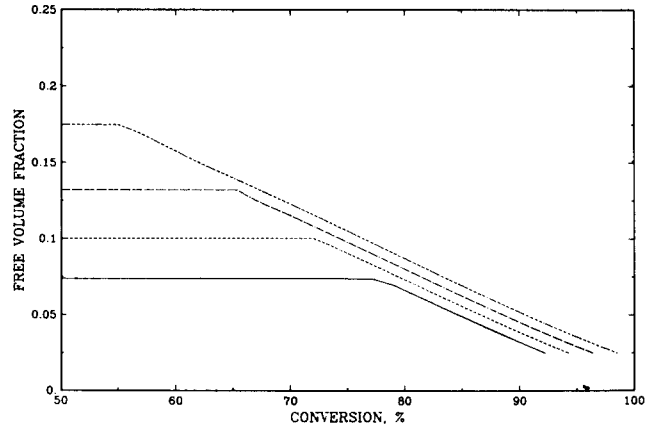


**Figure 23** Free volume fraction of polymer phase *versus* conversion at different temperatures: ———, 40°C; ---, 50°C; ———, 60°C; ————————, 70°C

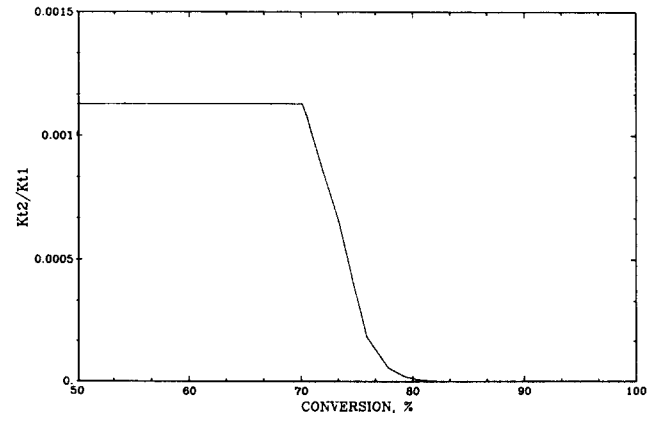


**Figure 24** Termination rate constant *versus* conversion at 50°C

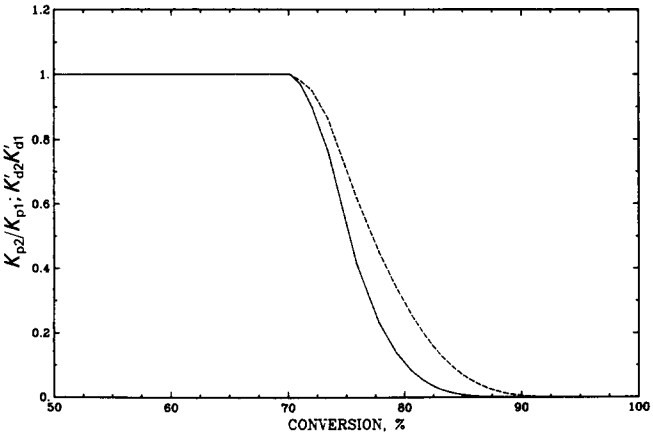


**Figure 25** $K_p$ and $K'_d$ *versus* conversion at 50°C: ———, $K_{p2}/K_{p1}$; – – – –, $K'_{d2}/K'_{d1}$

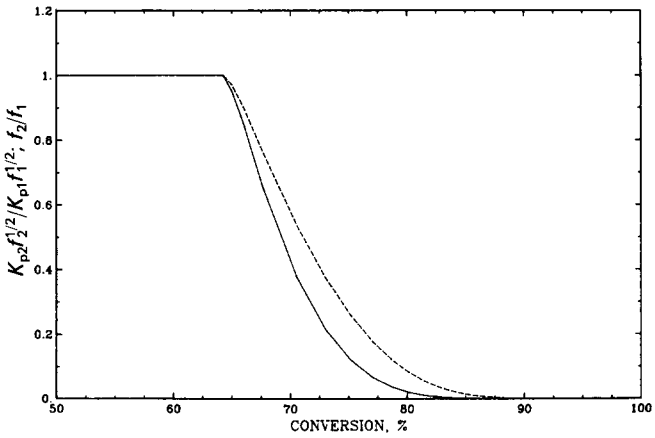


**Figure 26** $K_p$ and $f$ *versus* conversion at 60°C: ———, $(K_p f^{1/2})_2/(K_p f^{1/2})_1$; – – – –, $f_2/f_1$

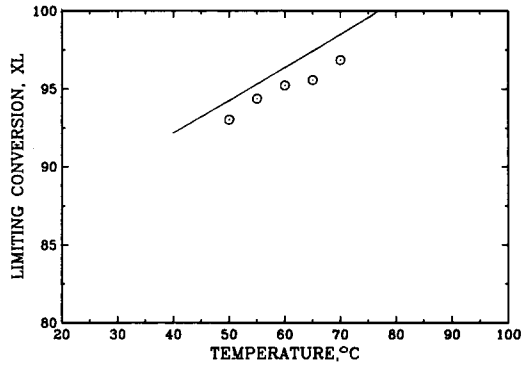


**Figure 27** Limiting conversion *versus* polymerization temperature: ○, present experimental data; ———, model

temperature of PVC. Practically, the 100% conversion cannot be obtained even for temperatures $> T_{gp}$ of PVC. *Figure 7* shows a typical run at 80°C, a temperature which is higher than $T_{gp}$ of PVC produced at this temperature. One can see from *Figure 7* that the model does not fit the experimental data at high conversions. The final conversion measured by gravimetry is lower than that expected. In fact, the PVC produced at this temperature is pink rather than the normal white. The dehydrochlorination rate of this PVC is much higher than that of ordinary PVC produced at lower polymerization temperature. Therefore, at high temperature and at high conversions, the VCM polymerization mechanism may be more complicated than accounted for in the model.

The parameter estimation and kinetic properties of VCM polymerization have been discussed above. *Figures 3–6* only show that the present model can fit the experimental data satisfactorily over the entire conversion range and cannot predict the reliability of the parameters discussed above. To evaluate the reliability of the present model further, we compared the model prediction by using the parameters mentioned above and individual experimental conditions with different experimental data measured by gravimetry as shown in *Figures 28–30*. These experimental data were obtained in three laboratories (MIPPT, AKZO and Zhejiang University) independently with different sized reactors and polymerization recipes. In *Figure 28*, one set of data was obtained by stopping the reaction at different times in our laboratory; the other set of data was measured by AKZO with a different reaction recipe. The data in *Figures 29* and *30* were obtained by gravimetry in a smaller reactor with different operation conditions and reaction recipe[84].

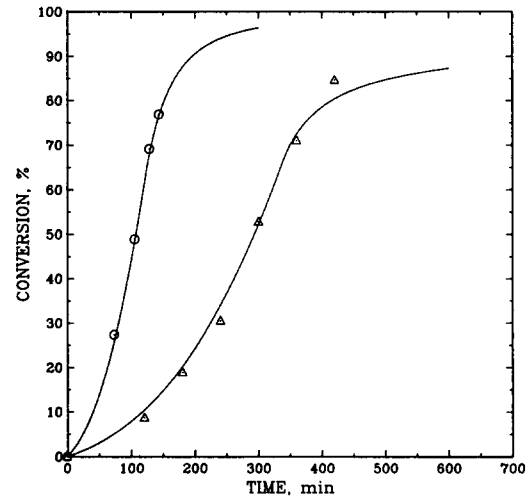


**Figure 28** Model prediction for suspension polymerization of vinyl chloride under different conditions: ○, present work, 5 l reactor, VCM 1116 g, water 2232 g; Perkadox 16-W40, [I] = 0.125 wt% at 60°C; △, AKZO data, 5 l reactor, VCM 675 g, water 2700 g, Perkadox-26, [I] = 0.0853 wt% at 53.5°C; ———, model prediction

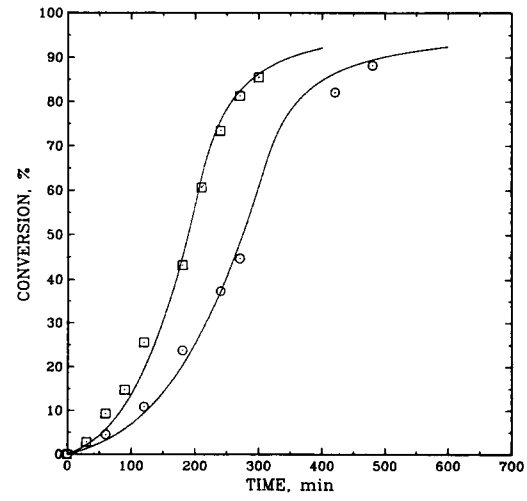


**Figure 29** Model prediction for suspension polymerization of vinyl chloride at different temperatures: 0.20 l reactor, VCM 40 g, water 80 g; AIBN, [I] = 0.16 wt%; □, 62°C; ○, 57°C; ———, model prediction

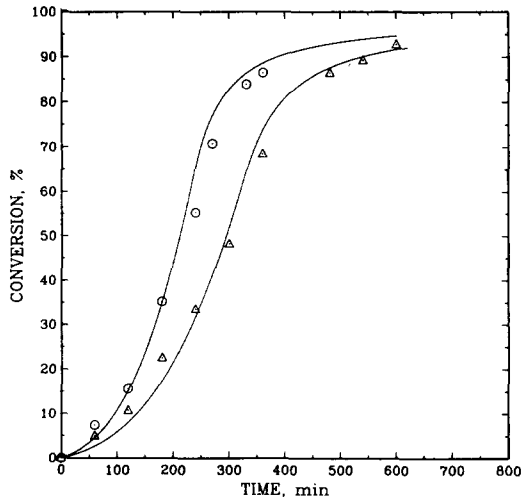


**Figure 30** Model prediction for suspension polymerization of vinyl chloride at 60°C: 0.20 l reactor, VCM 40 g, water 80 g, initiator AIBN; ○, 0.16 wt%; △, 0.09 wt%; ———, model prediction

Considering the accuracy of each batch by gravimetry, one can see that the model prediction is in excellent agreement with the experimental results. This not only proves the reliability of the model parameters estimated but also suggests that the type of suspending agent and conditions of mixing may not affect the kinetic behaviour significantly. It is believed that the present model should find use in the design, optimization and control of PVC reactor.

## CONCLUSIONS

A comprehensive kinetic model which applies over the entire conversion range (to limiting conversion) and a useful temperature range has been developed. The model prediction is in excellent agreement with independent experimental results with different reactor operation conditions and chemical recipe.

The present model can describe the main features of two-phase polymerization quantitatively. Radical transfer from phase to phase may not be governed by the mass transfer process and it depends on the nature of VCM polymerization. Precipitation of radical from the monomer phase can be expressed as a parameter $K^*$ which depends on temperature. The modified desorption rate constant $K'_{de}$ depends on both temperature and particle size. Radical exchange between two phases is significant only at very low conversions. The partition coefficient of initiator is $\approx 0.77$ and is independent of temperature and the nature of initiator. The concentration of radicals in the polymer phase is $\approx 30$ times that in the monomer phase at 50°C. The acceleration behaviour of VCM polymerization rate continues until conversion is near $X_f$ for the normal polymerization but the peak rate depends on initiator half life and concentration used.

The bimolecular termination reaction in the polymer phase is diffusion controlled over the entire conversion range. The propagation reaction becomes diffusion controlled and the initiator efficiency falls dramatically after the monomer phase is consumed. The initiation mechanism for high conversions depends on the nature of the initiator. The initiator efficiency for AIBN and the effective decomposition rate constant for peroxide initiator decrease significantly at high conversions.

VCM polymerization above the glassy state transition temperature of PVC involves a more complicated reaction mechanism. Pink PVC products were obtained for polymerization temperatures above 70°C.

## ACKNOWLEDGEMENTS

Financial support from the National Sciences and Engineering Research Council of Canada and the McMaster Institute for Polymer Production Technology is appreciated.

## REFERENCES

1 Rigo, A., Palma, G. and Talamini, G. *Macromol. Chem.* 1972, **152**, 219
2 Bezdaea, E. C., Buruiana, E. C., Istrate-Robila, G. and Caraculacu, A. A. *Eur. Polym. J.* 1973, **9**, 445
3 Bovey, F. A., Abbas, K. B., Schilling, F. C. and Starnes, W. H. Jr. *Macromolecules* 1975, **8**, 437
4 Starnes, W. H. Jr., Schilling, F. C., Abbas, K. B., Cais, R. E. and Bovey, F. A. *Macromolecules* 1979, **12**, 556
5 Starnes, W. H. Jr., Schilling, F. C., Abbas, K. B., Cais, R. E. and Bovey, F. A. *Polym. Prepr.* 1979, **20**, 653
6 Starnes, W. H. Jr., Schilling, F. C., Plitz, I. M., Cais, R. E., Freed, D. J., Hartless, R. L. and Bovey, F. A. *Macromolecules* 1983, **16**, 790
7 Hjertberg, T. and Sorvik, E. M. *J. Macromol. Sci. Chem.* 1982, **A17**, 983
8 Hjertberg, T. and Sorvik, E. M. *Polymer* 1983, **24**, 673
9 Hjertberg, T. and Sorvik, E. M. *Polymer* 1983, **24**, 685
10 Talamini, G. *J. Polym. Sci. A-2* 1966, **4**, 535
11 Crosato-Arnaldi, A., Talamini, G. and Vidotto, G. *Makromol. Chem.* 1968, **111**, 123
12 Ugelstad, J., Lervik, H., Gardinovacki, B. and Sundo, E. *Pure Appl. Chem.* 1971, **26**, 121
13 Abdel-Alim, A. H. and Hamielec, A. E. *J. Appl. Polym. Sci.* 1972, **16**, 783
14 Kuchanov, S. J. and Bort, D. N. *Polym. Sci. USSR* 1973, **15**, 2712
15 Olaj, O. F. *J. Macromol. Sci. Chem.* 1977, **A11**, 1307
16 Suresh, A. K. and Chanda, M. *Eur. Polym. J.* 1982, **18**, 607
17 Kelsall, D. K. and Maitland, G. C. 'Polymer Reaction Engineering' (Eds. K. H. Reichert and W. Geiseler), Hanser, Munich, 1983, p. 131
18 Lewis, J., Okiemen, F. E. and Park, G. S. *J. Macromol. Sci. Chem.* 1982, **A17**, 1021
19 Marinin, V. G., Bort, D. N., Zhil'tsov, V. V., Kuchanov, S. I., Ivereva, G. F. and Rybkin, E. P. *Polym. Sci. USSR* 1980, **22**, 261
20 Nass, L. I. 'Encyclopedia of PVC' (Ed. L. I. Nass), Vol. 1, Marcel Dekker, New York, 1976, p. 271
21 Enomoto, S. *J. Polym. Sci. A-1* 1969, **7**, 1255
22 Bengough, W. I. and Norrish, R. G. W. *Proc. R. Soc. Lond.* 1950, **A200**, 301
23 Cotman, J. D. Jr. *Ann. NY Acad. Sci.* 1953, **57**, 417
24 Burnett, G. M. and Wright, W. W. *Proc. R. Soc. Lond.* 1954, **A221**, 37
25 Mickley, H. S., Michaels, A. S. and Moore, A. L. *J. Polym. Sci.* 1962, **60**, 121
26 Marzurek, V. V. *J. Polym. Sci.* 1966, **8**, 1292
27 Park, G. S. and Smith, D. G. *Trans. Faraday Soc.* 1969, **65**, 1854
28 Talamini, G. and Peggion, E. 'Vinyl Polymerization' (Ed. G. Ham), Vol. 1, Marcel Dekker, New York, 1967, p. 331
29 Caraculacu, A. and Buruiana, E. C. *J. Polym. Sci., Polym. Chem. Edn.* 1978, **16**, 2741
30 Caraculacu, A., Buruiana, E. C. and Robila, G. *J. Polym. Sci., Polym. Symp.* 1978, **64**, 189
31 Park, G. S. *J. Vinyl Technol.* 1985, **7**, 60
32 Darricades-llauro, M. F., Michel, A. and Guyot, A. *J. Macromol. Sci. Chem.* 1986, **A23**, 221
33 Starnes, W. H. Jr. *Polym. Prepr.* 1977, **18**, 493
34 Bovey, F. A., Schilling, F. C., Starnes, W. H. Jr. *Polym. Prepr.* 1979, **20**, 160
35 Starnes, W. H. Jr. 'Developments in Polymer Degradation' (Ed. M. Grassie), Vol. 3, Applied Science, London, 1981, p. 135
36 Razuvyev, G. A., Petukhov, G. G. and Dodonov, V. A. *Polym. Sci. USSR* 1963, **3**, 1020

37 Park, G. S. and Smith, D. G. *Makromol. Chem.* 1970, **131**, 1
38 Hjertberg, T., Sorvik, E. and Wendel, A. *Makromol. Chem. Rapid Commun.* 1983, **4**, 175
39 Caraculacu, A. A. *Pure Appl. Chem.* 1981, **53**, 385
40 Okieimen, E. F. *Eur. Polym. J.* 1981, **17**, 641
41 Okieimen, E. F. *Eur. Polym. J.* 1983, **19**, 255
42 Okieimen, E. F. *J. Macromol. Sci. Chem.* 1983, **20**, 711
43 Cotman, J. D., Gonzalez, M. F. and Claver, G. C. *J. Polym. Sci. A-1* 1967, **5**, 1137
44 Bort, D. N., Rylov, Ye. Ye., Okladnov, N. A., Shtarkman, B. P. and Kargin, V. A. *Polym. Sci. USSR* 1965, **7**, 50
45 Bort, D. N., Marinin, V. G., Kalinin, A. I. and Kargin, V. A. *Polym. Sci. USSR* 1967, **9**, 334
46 Bort, D. N., Marinin, V. G., Kalinin, A. I. and Kargin, V. A. *Polym. Sci. USSR* 1968, **10**, 2989
47 Barrclay, L. M. *Angew. Makromol. Chem.* 1976, **52**, 1
48 Boissel, J. and Fischer, N. *J. Macromol. Sci. Chem.* 1977, **11**, 1249
49 Zichy, E. L. *J. Macromol. Sci. Chem.* 1977, **A11**, 1205
50 Wilson, J. C. and Zichy, E. L. *Polymer* 1979, **20**, 264
51 Cooper, W. D., Speirs, R. M., Wilson, J. C. and Zichy, E. L. *Polymer* 1979, **20**, 265
52 Rance, D. G. and Zichy, E. L. *Polymer* 1979, **20**, 267
53 Davidson, J. A. and Witenhafer, D. E. *J. Polym. Sci., Polym. Phys. Edn.* 1980, **18**, 51
54 Rance, D. G. and Zichy, E. L. *Pure Appl. Chem.* 1981, **53**, 377
55 Willmouth, F. M., Rance, D. G. and Henmean, K. M. *Polymer* 1984, **25**, 1185
56 Tornell, B. E. and Uustalu, J. M. *J. Vinyl Technol.* 1982, **4**, 53
57 Tornell, B. E. and Uustalu, J. M. *Polymer* 1986, **27**, 250
58 Tornell, B. E., Uustalu, J. M. and Jonsson, B. *Colloid Polym. Sci.* 1986, **264**, 439
59 Nilsson, H., Silvegren, C. and Uustalu, J. *Polym. Commun.* 1983, **24**, 268
60 Ravey, M., Waterman, J. A., Shorr, L. M. and Kramer, M. *J. Polym. Sci., Polym. Chem. Edn.* 1974, **12**, 2821
61 Fisher, N. *J. Vinyl Technol.* 1984, **6**, 35
62 Feldman, D., Macoveanu, M. and Robila, G. *J. Macromol. Sci. Chem.* 1977, **A11**, 1333
63 Soni, P. L., Geil, P. H. and Collins, E. A. *J. Macromol. Sci. Phys.* 1981, **B20**, 479
64 Tornell, B. and Uustalu, J. *J. Appl. Polym. Sci.* 1988, **35**, 63
65 Palma, G., Talamini, G. and Tavan, M. *J. Polym. Sci., Polym. Phys. Edn.* 1977, **15**, 1537
66 Smallwood, P. V. *Polymer* 1986, **27**, 1609
67 Allsopp, M. W. *Pure Appl. Chem.* 1981, **53**, 449
68 Allsopp, M. W. 'Manufacture and Processing of PVC' (Ed. R. H. Burgess), Applied Science, London, 1982, p. 151
69 Meeks, M. R. *Polym. Eng. Sci.* 1969, **9**, 141
70 Nilsson, H., Silvegren, C. and Tornell, B. *Angew. Makromol. Chem.* 1983, **112**, 125
71 Crosato-Arnaldi, A., Gasparini, P. and Talamini, G. *Makromol. Chem.* 1968, **117**, 140
72 Abdel-Alim, A. H. and Hamielec, A. E. *J. Appl. Polym. Sci.* 1974, **18**, 1603
73 Ugelstad, J., Mork, P. C., Dahl, P. and Pangnes, P. *J. Polym. Sci.* 1969, **C27**, 47
74 Russo, S. and Stannett, V. *Makromol. Chem.* 1971, **143**, 47
75 Arlman, E. J. and Wagner, W. M. *J. Polym. Sci.* 1952, **9**, 561
76 Bankoff, S. G. and Shreve, R. N. *Ind. Eng. Chem.* 1953, **45**, 270
77 Talamini, G. and Vidotto, G. *Makromol. Chem.* 1961, **50**, 129
78 Talamini, G. and Vidotto, G. *Makromol. Chem.* 1962, **53**, 21
79 Ryska, M., Kolinsky, M. and Lim, D. *J. Polym. Sci.* 1967, **C16**, 621
80 Farber, E. and Koral, M. *Polym. Eng. Sci.* 1968, **8**, 11
81 Tavan, M., Pulnia, G., Carenza, M. and Brugnaro, S. *J. Polym. Sci., Polym. Chem. Edn.* 1974, **12**, 411
82 Ugelstad, J., Flogstad, H., Hertzberc, T. and Sund, E. *Makromol. Chem.* 1973, **164**, 171
83 Ugelstad, J. *J. Macromol. Sci. Chem.* 1977, **A11**, 1281
84 Xie, T. Y., Yu, Z. Z., Cai, Q. Z. and Pan, Z. R. *Huangong Xuebao* 1984, **2**, 93
85 Xie, T. Y., Hamielec, A. E., Wood, P. E. and Woods, D. R. J. *Appl. Polym. Sci.* 1987, **34**, 1749
86 Vidotto, G., Brugnaro, S. and Talamini, G. *Makromol. Chem.* 1971, **140**, 249
87 Russo, S. and Stannett, V. *Makromol. Chem.* 1971, **143**, 57
88 Pezzin, G., Talamini, G. and Vidotto, G. *Makromol. Chem.* 1961, **43**, 12
89 Sorvik, E. M. *J. Polym. Sci., Polym. Lett. Edn.* 1976, **14**, 735
90 Hamielec, A. E., Gomez-Vaillard, R. and Marten, F. L. *J. Macromol. Sci. Chem.* 1982, **A17**, 1005
91 Hjertberg, T. and Sorvik, E. M. 'Degradation and Stabilisation of PVC' (Ed. E. D. Owen), Elsevier Applied Science, London, 1984, p. 21
92 Bueche, F. 'Physical Properties of Polymers', Wiley–Interscience, New York, 1962
93 Flory, P. J. 'Principles of Polymer Chemistry', Cornell University Press, Ithaca, New York, 1953
94 Xie, T. Y., Hamielec, A. E., Wood, P. E. and Woods, D. R. 'Experimental investigation of vinyl chloride polymerization at high conversion – conversion and tracer response relationships', *J. Appl. Polym. Sci.* 1990, **41**, 2327
95 Fedors, R. J. *J. Polym. Sci., Polym. Lett. Edn.* 1979, **17**, 719
96 Reding, F. P., Walter, E. R. and Welch, F. J. *J. Polym. Sci.* 1962, **56**, 225
97 Ceccorulli, G., Pizzcli, M. and Pezzin, G. *J. Macromol. Sci. Phys.* 1977, **B14**, 499
98 Friis, N. and Hamielec, A. E. 'Emulsion Polymerization' (Eds. I. Piirma and J. L. Gardon), *ACS Symp. Ser.* 1976, **24**, 82
99 Berens, A. R. *Org. Coat. Plast. Chem.* 1978, **39**, 236
100 Ibragimov, I. Y. and Bort, D. N. *Vysok. Soed. B* 1974, **16**, 376
101 Bawn, C. E. H. and Mellish, S. F. *Trans. Faraday Soc.* 1951, **47**, 1216
102 Van Hook, J. P. and Tobolsky, A. V. *J. Am. Chem. Soc.* 1958, **80**, 779
103 Barrett, K. E. *J. Appl. Polym. Sci.* 1967, **11**, 1617
104 Talat-Erben, M. and Bywater, S. *J. Am. Chem. Soc.* 1955, **77**, 3712
105 Lewis, R. and Friedman, R. *Modern Plastics* March 1973, 88
106 Pan, Z. R. and Yu, Z. Z. 'Free Radical Polymerization', Chemical Industry Press, Beijing, 1983, p. 84
107 Westmijze, H. AKZO Chemie, Noury Initiators, personal communication, 1987
108 Arnett, L. M. and Peterson, J. H. *J. Am. Chem. Soc.* 1952, **74**, 2031
109 Mazurek, V. V. *Polym. Sci. USSR* 1966, **8**, 1292
110 Olaj, O. F., Breitenbach, J. W., Parth, K. J. and Philippovich, N. *J. Macromol. Sci. Chem.* 1977, **A11**, 1319
111 Burnett, G. M. and Wright, W. W. *Proc. R. Soc. Lond.* 1954, **A221**, 28
112 Nomura, M. 'Emulsion Polymerization' (Ed. I. Piirma), Academic Press, New York, 1982


## NOMENCLATURE

| | |
|---|---|
| $A^*$ | Free volume factor used in $K_t$ equation |
| $B^*$ | Free volume factor used in $K_p$ equation |
| $B_f^*$ | Free volume factor used in $K_p f^{1/2}$ equation |
| $C^*$ | Free volume factor used in $K_d'$ equation |
| $C_M$ | Ratio of $K_{fm}$ to $K_p$ |
| $d_p$ | Diameter of primary particle, d*m* |
| $D_{g0}$ | Vapour density at vapour pressure ($g\,l^{-1}$) |
| $D_m$ | Density of monomer ($g\,l^{-1}$) |
| $D_p$ | Density of polymer ($g\,l^{-1}$) |
| $D_w$ | Density of water ($g\,l^{-1}$) |
| $f$ | Initiator efficiency |
| I | Initiator |
| [I] | Concentration of initiator ($mol\,l^{-1}$) |
| $J$ | Parameter defined in the model |
| $K$ | Solubility constant of VCM in water |
| $K^*$ | Parameter of precipitation defined in the model |
| $K_d$ | Decomposition rate constant of initiator ($s^{-1}$) |
| $K_{de}$ | Desorption rate constant of radicals |
| $K_D$ | Rate constant of primary radical diffusion out from cage |
| $K_{R1}$ | Rate constant of inert formation in cage |
| $K_{R2}$ | Rate constant of recombination in cage |
| $K_x$ | Rate constant of radical pair reacting with monomer in cage |
| $K_{fm}$ | Chain transfer to monomer rate constant ($l\,mol^{-1}\,s^{-1}$) |

$K_{fp}$ Chain transfer to polymer rate constant ($l\ mol^{-1}\ s^{-1}$)
$K_i$ Initiation rate constant ($l\ mol^{-1}\ s^{-1}$)
$K_p$ Propagation rate constant ($l\ mol^{-1}\ s^{-1}$)
$K_t$ Termination rate constant ($l\ mol^{-1}\ s^{-1}$)
$K_{1-5}$ Reaction rate constant defined in reaction (4)–(8)
$K_I$ Initiator partition coefficient
M Monomer
$M_1$ Monomer in the monomer phase (g)
$M_2$ Monomer in the polymer phase (g)
[M] Concentration of monomer ($mol\ l^{-1}$)
$M_g$ Monomer in the gas phase (g)
$M_{gX_f}$ Monomer in the gas phase at $X_f$ (g)
$M_m$ Molecular weight of monomer
$M_0$ Initial monomer charged (g)
$M_w$ Monomer in the water phase (g)
$N_m$ Mole number of monomer
$P_m$ Partial pressure of monomer (atm)
$P_m^\circ$ Vapour pressure of monomer (atm)
$(Q_1)$ Polymer concentration ($mol\ units\ l^{-1}$)
$r_c$ Critical chain length to precipitate
$R$ Gas constant ($l\ atm\ mol^{-1}\ K^{-1}$ or $cal\ mol^{-1}\ K^{-1}$)
$R_I$ Initiation rate ($mol\ l^{-1}\ s^{-1}$)
$R_r^\bullet$ Radical with chain length $r$
$[R^\bullet]$ Radical concentration ($mol\ l^{-1}$)
$R_i^\bullet$ Primary radical
$t$ Reaction time (min) or temperature (°C)
$T$ Temperature (K)
$T_{gm}$ Glassy transition temperature of monomer
$T_{gp}$ Glassy transition temperature of polymer
$V$ Reaction volume (l)
$V_r$ Reactor volume (l)
$W_w$ Water charged (g)
$X$ Fraction conversion
$X_f$ Critical conversion at which the monomer phase is consumed
$X_L$ Limiting conversion

*Greek letters*

$\alpha_m$ Thermal expansion factor for VCM
$\alpha_p$ Thermal expansion factor for PVC
$\phi_p$ Volume fraction of polymer in the polymer phase
$\phi_2$ Volume fraction of polymer phase
$\chi$ VCM–PVC interaction parameter

*Subscripts*

0 Initial state
1 Monomer phase
2 Polymer phase
m Monomer
p Polymer